Electrical Engineering Kaleidoscope

EEK 2006

A PUBLICATION OF THE ELECTRICAL ENGINEERING DEPARTMENT UNIVERSITY OF WASHINGTON

ANNUAL RESEARCH REVIEW

Calling all EE alumni. This party's for you!

Saturday, April 29, 2006

Your alma mater is celebrating 100 years and you're invited! We have a fantastic line-up of events including a keynote address by Bernard S. Meyerson, a vice president of IBM's Systems and Technology Group, lab tours with a preview of emerging technology, and a celebration dinner with live music. Best of all, you'll have a chance to reconnect with former classmates, professors, and friends.

There's more ... Also on Saturday, the whole family will enjoy our free Engineering Open House featuring hundreds of interactive exhibits for all ages. Live entertainment, lectures, art displays, and various demonstrations will be happening all over campus for the annual Washington Weekend event. There will be something for everyone! We hope to see you in April.

UNIVERSITY of WASHINGTON COLLEGE of ENGINEERING *Electrical Engineering*

CELEBRATING 100 YEARS 100

Don't miss it! Register online today.

It's fast. It's easy. It's secure.
www.ee.washington.edu/centennial

Need more info?
Contact the University of Washington Alumni Association 206.543.0540

UW ALUMNI ASSOCIATION

EEK2006

ANNUAL RESEARCH REVIEW

CONTENTS...

WELCOME TO EEK2006

The previous two issues of EEK examined the past and future of Electrical Engineering. This year's edition is particularly unique because it showcases the cutting edge research being performed by our future electrical engineering faculty and industry leaders—our students and post docs. These are the faces that will lead the next generation in fulfilling our mission of Excellence in Education Through Cutting Edge Research.

Consequently, they will also be the ones to continue UWEE's long legacy of innovation. We will recognize A Century of Innovation on April 29th, 2006 as part of the department's Centennial Celebration. Please come celebrate with us. For more information about UW EE's Centennial Celebration, feel free to contact: centennial@ee.washington.edu.

DAVID J. ALLSTOT
Chair and Boeing-Egtvedt Professor
Department of Electrical Engineering

PUBLISHER
Electrical Engineering Department of the University of Washington
Dave Allstot, Chair
Sumit Roy, Associate Chair for Research & Development
Leung Tsang, Associate Chair for Education

DESIGN STAFF
Sarah Conradt, Designer

EDITORIAL STAFF
Howard Chizeck, Faculty Editor
Laura Haas, Staff Editor

Print management by University of Washington Publications Services

Video Tooning

JUE WANG, GRADUATE STUDENT (EE)

Animated imagery brings life to the screen. The stylized abstraction of reality one sees in animation adds an immediate impact that cannot be captured by simply pointing a video camera at a scene. But such animation is both labor intensive and requires considerable artistic skill.

A “Video Tooning” system has been developed to transform an input video into space-time volume of image data. Optimization algorithms are efficiently employed to quickly cut out and stylize video objects into a cartoon-like style. Instead of processing a video frame-by-frame, this system accumulates the video frames to create a 3-D data volume and directly processes the pixels in 3-D space (x, y, t).

The system is composed of two main components: an interactive foreground extraction and a stylized video rendering. Given an input video, the system first provides an efficient tool to allow users to quickly extract the dynamic foreground object. To achieve this, a novel painting-based user interface has been developed to allow users to easily indicate the foreground object across space and time.

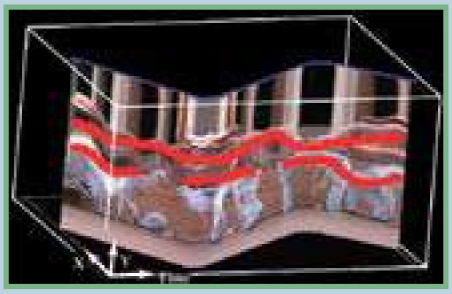

A PAINTING-BASED USER INTERFACE HAS BEEN CREATED FOR THIS SYSTEM THAT ALLOWS THE USER TO EASILY INDICATE THE FOREGROUND OBJECT (IN THIS EXAMPLE, THE SKATEBOARDER) ACROSS SPACE AND TIME.

THE SKATEBOARDER, THE ELEPHANT AND THE BALLET DANCER ARE EXTRACTED FROM THREE SOURCE VIDEOS (LEFT) AND COMPOSED TOGETHER IN FRONT OF THE STUDENT CENTER AT UW (RIGHT).

THIS SYSTEM PROVIDES STYLIZATION TOOLS TO CONSISTENTLY TRANSFER THE SKATEBOARDER INTO CARTOON STYLE THROUGH THE WHOLE VIDEO.

Also, a new hierarchical video segmentation algorithm is proposed; it combines multiple optimization algorithms to quickly segment the foreground object, typically in ten seconds for a 200 frame video.

Extracted foreground objects from different source videos can be composed together to create special visual effects.

Furthermore, this system provides a variety of rendering tools to stylize the spatio-temporal foreground object and create a highly abstract cartoon with temporal coherence.

Future plans are to improve the user interface and make it possible to create other animation styles. Another goal is to make the program work better with hand-held cameras.EE

FACULTY ADVISOR: PROFESSOR EVE A. RISKIN
COLLABORATORS: MICHAEL F. COHEN (MICROSOFT RESEARCH), PROFESSOR RICHARD LADNER (CSE)
RESEARCH AREA: IMAGE AND VIDEO PROCESSING
GRANT/FUNDING SOURCE: MICROSOFT

Improving Hearing Aids Through Modulation Filtering

STEVEN SCHIMMEL, GRADUATE STUDENT (EE)

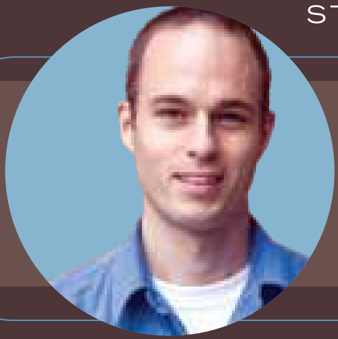

Users of hearing devices commonly complain that they are unable to focus on a single talker in situations with many interfering talkers. Hearing devices augmented with modulation filtering overcome this problem by selectively amplifying only the talker of interest.

Current hearing aids amplify all incoming sounds in equal fashion. This works fine when there's only a single talker, but it is detrimental to intelligibility in the presence of many interfering talkers, like in a restaurant or at a cocktail party. To be useful in those situations, hearing aids such as conventional behind-the-ear hearing aids and cochlear implants, must distinguish between the desired talker and the background babble.

CURRENT HEARING AIDS AMPLIFY ALL SOUNDS EQUALLY. WITH MODULATION FILTERING, ONLY THE SIGNAL OF INTEREST IS SELECTED AND AMPLIFIED.

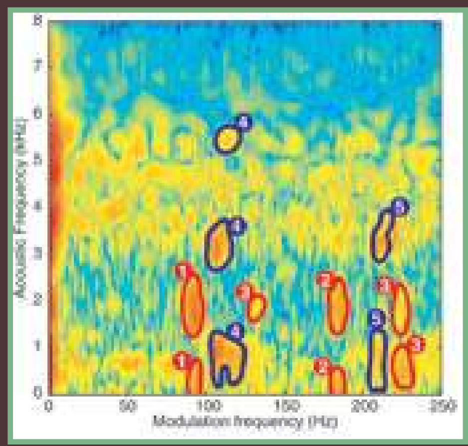

ELEMENTS OF THE MODULATION SPECTROGRAM THAT REPRESENT FEATURES OF INDIVIDUAL SPEAKERS PRESENT IN THE SIGNAL. NUMBERS 1-3 REPRESENT PITCH FUNDAMENTAL, PITCH HARMONIC AND ALIASED PITCH OF THE FIRST SPEAKER, WHILE NUMBERS 4-5 REPRESENT PITCH FUNDAMENTAL AND PITCH HARMONIC FOR THE SECOND SPEAKER.

Through the use of a signal processing technique called modulation filtering, a hearing aid can separate the desired talker from background noise using the modulation spectrogram representation of the input signal. It then can filter out the signal of interest with a modulation filter that is tuned to the desired talker.

In a preliminary subjective listening test, a prototype of this proposed algorithm significantly improved speech intelligibility.

This research can help users of hearing aids to focus on a single talker in situations with many interfering speech signals. As such, it contributes to the performance and usefulness of hearing aids in many everyday situations. EE

FACULTY ADVISOR: PROFESSOR LES ATLAS
COLLABORATORS: PROFESSOR PAM SOUZA (SPEECH & HEARING SCIENCES), JAY RUBINSTEIN (VMB HEARING RESEARCH CENTER)
RESEARCH AREA: DSP / HEARING AIDS
GRANT/FUNDING SOURCE: BLOEDEL HEARING INSTITUTE, GAP FUND, WASHINGTON RESEARCH FOUNDATION

PILOT: A Hierarchical Electromagnetic and Signal Integrity Simulator for Microelectronics and Beyond

SWAGATO CHAKRABORTY AND CHUANYI YANG, GRADUATE STUDENTS (EE)

Rapid increase in clock-speed and packaging density have increased the electromagnetic (EM) effects in cross-talk, substrate coupling and in the radiation of integrated circuits and packages. Consequently, accurate and efficient modeling is mandatory to maintain the desired level of signal integrity in emerging micro and nano electronic designs.

For years, boundary element-based solutions of Maxwell's equations were used. However, due to significant algorithmic and computational science breakthroughs, speed and memory efficiency required for simulation and design cycle acceleration of large-scale detailed electronic structures are now available.

The Applied Computational Electromagnetics Lab has developed an accelerated boundary element-based 3-D full-wave EM simulator named PILOT (Predetermined Interaction List Oct Tree). This simulator deals with the classical problem of dense matrices in boundary element techniques using a robust multi-level low-rank tree-based decomposition algorithm. This leads to an extremely fast matrix setup and a solution with linear complexity and memory use in problem size. PILOT is fully scalable on parallel architectures, and connects directly to circuit simulation tools. It can compute electromagnetic parasitics with more than a million unknowns in ten minutes, which is about 50 times faster than commercial technologies. PILOT also simulates complex microelectronic structures from the Air Force Research Labs, Hughes Research Labs, Intel, Mayo Foundation, Rockwell Scientific, Intel, IBM and NASA.

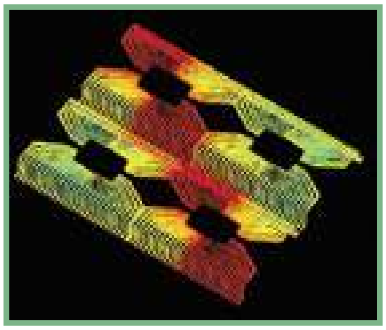

A CHARGE PLOT OF A DENSE PACKAGE LEADS STRUCTURE WHERE 28 LEADS WERE EXCITED. PILOT ENABLES S-PARAMETER COMPUTATION OF PACKAGE LEAD INTERACTION AND CROSSTALK, AND PERMITS CHIP-PACKAGE CO-SIMULATION.

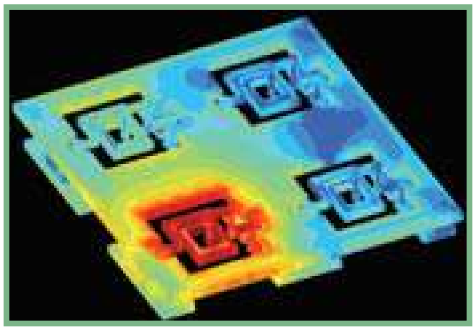

CURRENT PLOT OF A CO-PLANAR MULTIPLE INDUCTOR STRUCTURE; THE SPIRAL INDUCTOR AT THE LEFT CORNER WAS EXCITED. PILOT ENABLES QUALITY FACTOR AND CROSS-TALK SIMULATION FOR MULTIPLE INDUCTOR USE IN OSCILLATOR AND WIRELESS SYSTEM DESIGN.

The technology of PILOT enables rapid simulation of distributed effects in integrated systems. It is currently being enhanced for rapid multi-physics modeling. This will enable the high-impact simulation of mixed-technology systems involving microfluidics, biological systems interaction, quantum dots and electrical nanostructures. EE

FACULTY ADVISOR: PROFESSOR VIKRAM JANDHYALA
COLLABORATORS: DIPANJAN GOPE (INTEL CORPORATION)
RESEARCH AREA: COMPUTATIONAL ELECTROMAGNETICS
GRANT/FUNDING SOURCE: DARPA, NSF, INTEL, UW TGIF

Design of Distributed Energy Systems – Educational Analogies Derived from Computer Systems

HENRY LOUIE, GRADUATE STUDENT (EE)

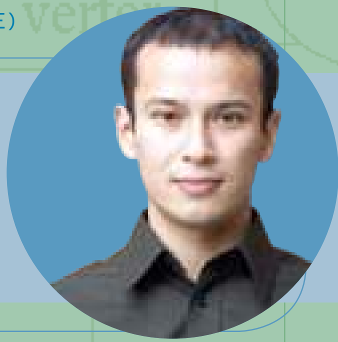

Computers integrate two data storage devices in their operation through cache control, which works by allocating data between the fast, expensive Random Access Memory (RAM), and the slow, inexpensive hard disk. The cache controller places frequently used data in the RAM, while storing the rest in the hard disk. This use of multi-level data storage results in a computer that is quick and has a large capacity.

An analogy between data and energy can be used to synthesize cache control for energy storage systems. Like RAM in data storage, energy storage devices such as flywheels have fast response times, but are expensive. An energy analogy of hard disks is hydrogen storage, which is inexpensive, but has a slow response time. Like a computer's use of RAM and hard disk, both energy storage device types can be used to achieve acceptable performance for a reasonable cost. This multi-level storage has an immediate application to wind power plants.

The variability of wind speed makes it impractical to schedule the power output of wind power plants. However, the integration of a multi-level energy storage system will allow a schedule to be followed.

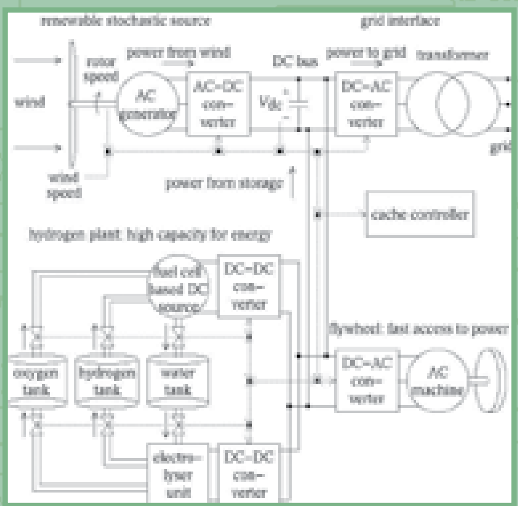

WIND POWER PLANT WITH MULTI-LEVEL ENERGY STORAGE.

The flywheel acts like RAM, absorbing or supplying the rapidly fluctuating portion of the power. The hydrogen storage through the use of a fuel cell or electrolyzer acts like a hard drive, accommodating the bulk of the power. The output of the power plant and the allocation of energy between devices are shown.

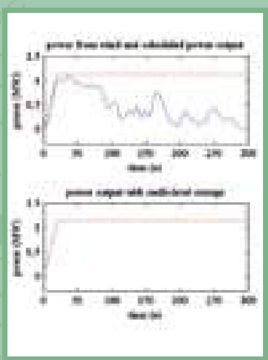

1

2

1. THE FIRST PLOT SHOWS A COMPARISON BETWEEN THE SCHEDULED POWER OUTPUT (DASHED LINE) AND THE POWER FROM THE WIND. THE SECOND PLOT INDICATES THAT WITH MULTI-LEVEL STORAGE, THE POWER OUTPUT CAN TRACE THE SCHEDULED POWER.

2. THE FIRST PLOT IS THE POWER REQUIRED FROM THE MULTI-LEVEL STORAGE. THE SECOND AND THIRD PLOTS SHOW POWER ALLOCATION BETWEEN THE FLYWHEEL AND FUEL CELL, RESPECTIVELY.

The strong analogy between data storage and energy storage at the device and functional level has been formed. This has been exploited for the synthesis of a multi-level energy storage system for use in a wind power plant. The value of the analogy as an instructional aid is currently being evaluated. EE

FACULTY ADVISOR: PROFESSOR KAI STRUNZ
RESEARCH AREA: POWER AND ENERGY SYSTEMS
GRANT/FUNDING SOURCE: ROYALTY RESEARCH FUND

Integrated Urban Hydrogen Power Park

ALEX ZHENG, UNDERGRADUATE (COMPUTER ENGINEERING)

A growing number of problems have surfaced in recent years due to fossil fuel consumption, motivating the energy industry to search for new alternatives. The need for a clean, easily generated, cost-effective replacement has encouraged continued research into the use of hydrogen fuel.

Traditionally, clean energy options have been very limited in urban areas. This project focuses on the need to bring clean, affordable hydrogen to such areas by creating a flexible, efficient system that uses a modular, vertically integrated design framework. By harnessing the untapped wind power on the roof of a skyscraper, a clean, renewable source of electricity was gained without creating a large footprint on valuable urban real estate. Four vertical-axis wind turbines were used to power a medium-sized hydrogen production operation.

The design was integrated with the skyscraper's electrical system, feeding excess electricity directly to the skyscraper or to the grid, and drawing grid power when wind power supplies were low. The advantages of a vertically integrated, modular design are in the ability to make efficient use of real estate and to customize the system to different areas and demands. An electrolyzer, compressor and several storage tanks are put in a previously unused basement, forming the production center. An electrolyzer generates hydrogen from electricity and water, which is then compressed for storage. The hydrogen is piped to a hydrogen dispenser where it is distributed. The design supports the fueling of 10 to 50 typical hydrogen cars a day.

This project received honorable mention at the 2005 international H2U Student Design Contest sponsored by the National Hydrogen Association, Chevron-Texaco and the U.S. Department of Energy. The team was recognized "for the brilliant innovation, technical aptitude and superior originality in the design of a next-generation hydrogen power park."EE

AN ILLUSTRATED EXAMPLE OF A SKYSCRAPER EQUIPPED WITH THE PROPOSED HYDROGEN PRODUCTION SYSTEM.

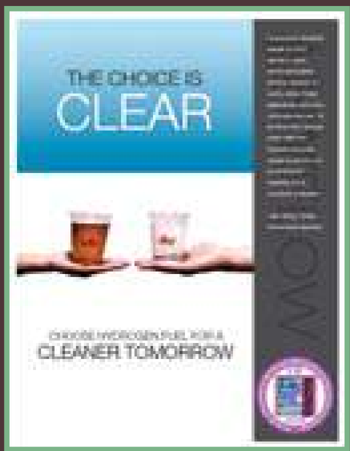

AN AD FOR A HYPOTHETICAL COMPANY THAT WAS DESIGNED FOR THE 2005 INTERNATIONAL H2U STUDENT DESIGN CONTEST.

FACULTY ADVISOR: PROFESSOR KAI STRUNZ
COLLABORATORS: TIMOTHY CHAO (BIOE), LIYANG CHEN (EE), JENNY LU (BUSINESS), GREG MARTIN (VISUAL COMMUNICATION DESIGN), CLINT NELSON (CIVILE), JUSTIN REED (EE), BRANDON RENFROW (COMPUTER SCIENCE)
RESEARCH AREA: WIND POWER AND HYDROGEN
GRANT/FUNDING SOURCE: NATIONAL SCIENCE FOUNDATION RESEARCH EXPERIENCES FOR UNDERGRADUATES

Locating Sensors among Adversaries – SeRLoc to the Rescue

LOUKAS LAZOS, GRADUATE STUDENT (EE)

Wireless sensor networks monitor physical properties in a Field of Interest (FoI) such as temperature, humidity and motion. In order to extract meaningful information from the collected observations, the sensed data must be correlated with space. When sensors are stochastically deployed, they must estimate their location via a process known as localization. This research focuses on the problem of providing secure localization services for wireless sensor networks.

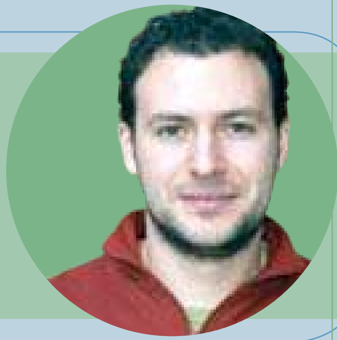

While sensor localization has been extensively explored for benign environments, enabling position estimation for sensors in the presence of adversaries has not been addressed. Attacks against the localization process not only disassociate the collected observations from the true location of sensors, but also inflict cross-layer vulnerabilities to location-dependent protocols of higher layers.

To ensure robust location estimation, a secure range-independent localization algorithm called SeRLoc was developed. SeRLoc relies on a two-tier network architecture. The network consist of a set of sensors of unknown location, and a set of nodes equipped with directional antennas called “locators,” with known location and orientation. Both the sensors and nodes are randomly deployed in the FoI. In SeRLoc, sensors passively estimate their position based on beacons transmitted from the locators. Each beacon contains localization information that defines the sector antenna where the beacon transmission took place. The center of gravity of the convex intersection of the sectors heard is chosen as the sensor location.

By analyzing the space of possible attacks against SeRLoc, we showed that cryptography alone is not sufficient to secure the localization process. Instead, lightweight cryptography was combined (such as hashing and symmetric encryption/decryption with deployment statistics) to allow sensors to detect attacks on the localization like the wormhole and Sybil attack. We also analytically evaluated the level of security achieved by SeRLoc using Spatial Statistics theory.

Securing the localization process is an essential requirement for providing secure network services. As the size of the sensor devices decreases, computational and energy resources become limited, so security becomes a challenging problem. To address this, secure localization methods that combine cryptography with multiple consistency checks on invariant physical properties must be developed. EE

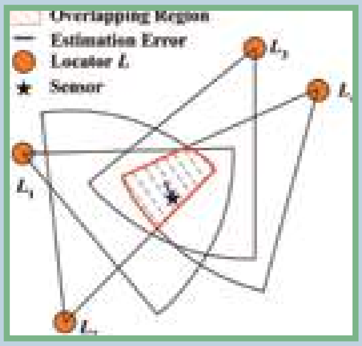

THE SENSOR DEFINES A SEARCH AREA WHERE IT WILL ATTEMPT TO LOCALIZE ITSELF BASED ON THE COORDINATES OF THE LOCATORS IT HEARS, AND THE COMMUNICATION RANGE R OF EACH LOCATOR. IT THEN PLACES A FINE GRID OF EQUALLY SPACED POINTS WITHIN THE SEARCH AREA.

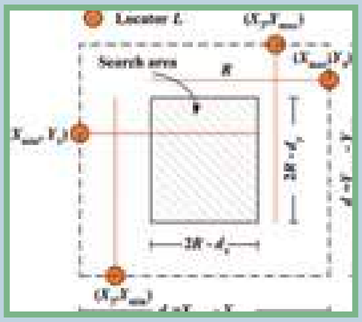

THE SENSOR PERFORMS A GRID-SECTOR TEST FOR EACH POINT OF THE SEARCH AREA AND FOR EACH LOCATOR. IF A POINT IS INCLUDED INSIDE A SECTOR, ITS VALUE ON A CORRESPONDING TABLE IS INCREASED BY ONE. THE DEFINED REGION OF INTERSECTION IS BASED ON MAJORITY VOTE.

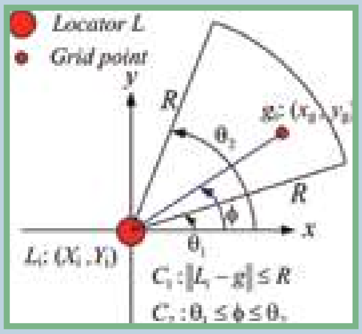

EACH LOCATOR BROADCASTS A BEACON CONTAINING THE COORDINATES AND SLOPES OF THE LINES THAT DEFINE THE SECTOR WHERE THE TRANSMISSION TAKES PLACE. THE SENSOR HEARS LOCATORS L_1 - L_4 AND ESTIMATES ITS LOCATION TO BE THE CENTER OF GRAVITY FOR THE REGION OF INTERSECTION.

FACULTY ADVISOR: PROFESSOR RADHA POOVENDRAN
RESEARCH AREA: SECURITY IN WIRELESS SENSOR NETWORKS
GRANT/FUNDING SOURCE: DEPARTMENT OF DEFENSE (DOD)

Privacy Protection of Electronic Healthcare in Multiuser Environments

MINGYAN LI, GRADUATE STUDENT (EE)

Privacy protection of electronic health records (EHR) has become a pressing social issue after the HIPAA (Health Insurance Portability and Accountability Act) took effect in April 2003. Though current research on privacy protection of medical images addresses secure storage and secure transmission before reception, authorized recipients can breach patient privacy by releasing medical images to unauthorized parties. Therefore, the ability to trace medical images is essential in order to prevent unauthorized image leakage.

Watermarking is one technique to trace unauthorized leakage of EHR back to the offenders. For tracing purposes, watermarking medical images must satisfy stringent fidelity requirements to ensure diagnostic quality and high robustness. Furthermore, groups of medical professionals often collaborate, making group communication a common practice in providing medical service.

Because of the nature of a multi-user clinical environment, an efficient watermarking scheme suitable for a many-to-many multicast scenario is proposed, where a broadcast copy is of diagnostic value only after being decoded by the authorized watermark key holders. During the process of decoding, two fingerprints are imprinted onto the image; one that corresponds to the original sender, and another that corresponds to the recipient performing the decoding.

This scheme is scalable in user storage and watermark key update communication. It requires only one watermark key to be stored by each user for each group, and no watermark key update is required when a member joins.

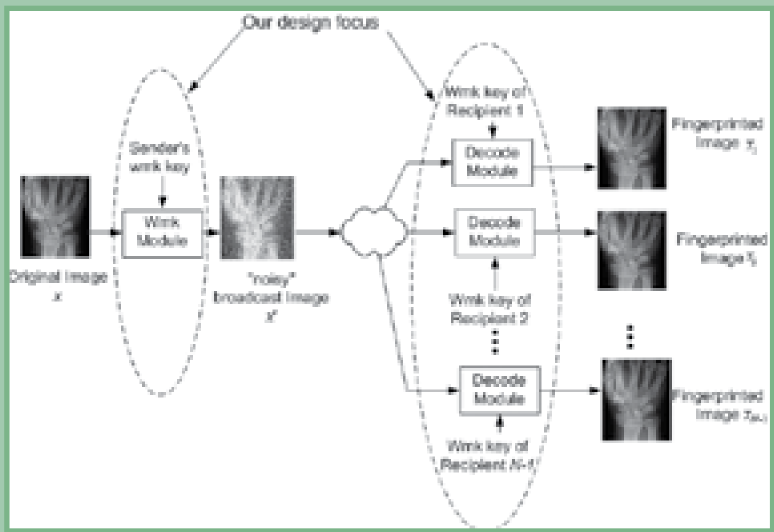

A PROPOSED FINGERPRINT MODEL THAT TRACES MEDICAL IMAGES WHILE MAKING USE OF COMMUNICATION EFFICIENCY OF A MULTICAST. NOTE THAT A BROADCAST IMAGE IS INTENTIONALLY "NOISY" TO ENFORCE THE DECODING PERFORMED BY RECIPIENTS BEFORE OBTAINING AN IMAGE OF DIAGNOSTIC VALUE. THE DECODING PROCESS EMBEDS THE WATERMARKS OF THE RECIPIENT'S AND THE SENDER'S TO A FINGERPRINTED IMAGE.

Simulation results conducted on 31 images of five modalities confirm that the fingerprinted images are of higher quality when compared to 10:1 JPEG compressed images, in terms of three image quality indices: peak signal to noise ratio (PSNR), quality index (QI) and mean squared Moran error (MSME). Meanwhile, the fingerprinted images withstand various image processing such as low pass filter (LPF), high pass filter (HPF), JPEG compression, cropping and averaging attack. EE

FACULTY ADVISOR: PROFESSOR RADHA POOVENDRAN
RESEARCH AREA: SECURITY AND PRIVACY IN MULTI-USER ENVIRONMENTS
GRANT/FUNDING SOURCE: NSF AND ARO

3-D Integrated Circuits

LILI ZHOU, CHERRY WAKAYAMA,
NUTTORN JANGKRAJARNG, BO HU, GRADUATE STUDENTS (EE)

3-D technology can potentially improve routing and area restrictions in current layout techniques. A 1024-bit fully parallel low-density parity-check (LDPC) code decoder has been designed and implemented using a 3-D CMOS technology. This 3-D decoder, with about 8M transistors, was designed to have a 2Gb/s throughput.

LDPC codes are emerging as standard methods of channel encoding and error correcting for many wireless standards due to their near Shannon-limit error correction performance. The LDPC block-parallel message passing decoding algorithm and its fully-parallel implementation architecture yield the high-throughput error-correction capability necessary for large-volume communication and data storage applications. However, the implementation also leads to challenges in hardware implementation, especially for large amounts of interconnection resources.

The 3-D circuit seen below is a promising technology that addresses interconnection issues.

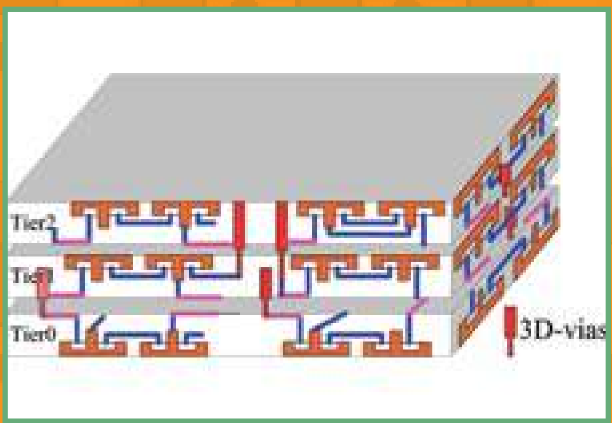

CROSS-SECTION OF THREE TIERS INTEGRATED TO FORM A 3-D CIRCUIT.

It is composed of multiple active circuit layers that are vertically stacked to allow shorter interconnection paths. However, because design methodologies and CAD tools for 3-D ASIC designs are immature or not readily available, 3-D placement tools have been developed. These tools can minimize the area, routing density, total wire length and 3D-via usage. Programs have also been created for 3-D routing, buffer insertion and circuit-versus-schematic (CVS) checking.

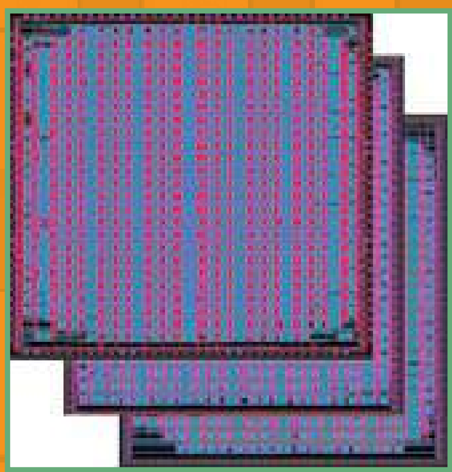

LAYOUT VIEW OF THE FINAL 3-TIER DESIGN.

The significance of this work is three-fold: (1) it is the first large-scale 3-D ASIC implementation, (2) 3-D IC process with three-tier integration was shown to yield an order of magnitude improvement over the corresponding 2-D process, in terms of power-delay-area product, and (3) an automated 3-D design flow has been developed and used to implement large-scale silicon ASIC design. EE

FACULTY ADVISOR: PROFESSOR RICHARD SHI
COLLABORATORS: MIT LINCOLN LAB
RESEARCH AREA: 3-D ASIC DESIGN AND CAD, LDPC DECODER DESIGN
GRANT/FUNDING SOURCE: DARPA AND SPAWAR

Calibration of Phased Arrays for High Data Rate Wireless Communications

CAMERON CHARLES, GRADUATE STUDENT (EE)

As wireless communications standards evolve, data rates increase significantly with each new generation. The 2G cellular standard accommodates data rates up to 20KBps, while the forthcoming 4G standard is expected to mandate data rates up to 1GBps. This trend forces engineers to find ways to increase data rates over wireless channels. As traditional time and frequency domain methods are exhausted, engineers are turning to spatial methods. One spatial method that shows great promise is the use of multiple-antenna transceivers.

A phased array is one type of multiple-antenna system, which transmits (or receives) the same signal on each antenna, but adjusts the relative phases and amplitudes. The constructive/destructive interference between these signals shapes the radiation into a beam. By adjusting the relative phases and amplitudes, the beam of radiated power can then be steered to "focus" it onto the desired user. This minimizes wasted power and increases the signal to noise ratio, thus enabling higher data rates.

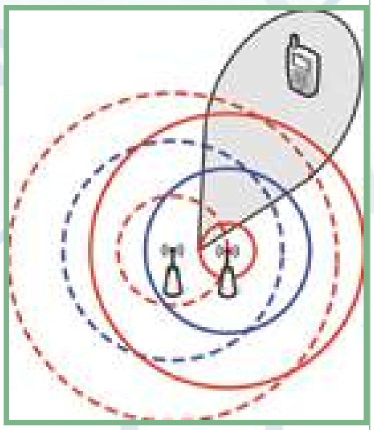

AN ILLUSTRATION OF A PHASED ARRAY TRANSMITTER IN OPERATION. THE ELECTROMAGNETIC RADIATION OF EACH ANTENNA IS DEPICTED BY THE CONCENTRIC RED AND BLUE CIRCLES (DENOTING THE WAVE MAXIMUMS AND MINIMUMS, RESPECTIVELY). CONSTRUCTIVE INTERFERENCE OCCURS WHERE THE COLORS COINCIDE RESULTING IN THE FORMATION OF A RADIATION BEAM (SHOWN IN GREY), WHICH CAN BE STEERED TOWARD THE DESIRED USER.

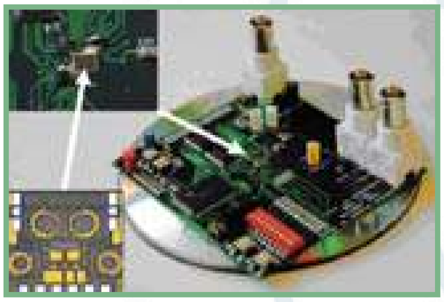

THE SYSTEM WILL BE TESTED USING A CHIP-ON-BOARD PACKAGING METHOD WHERE THE SILICON DIE IS WIRE-BONDED DIRECTLY TO A PRINTED CIRCUIT BOARD, ALLOWING MEASUREMENTS TO BE TAKEN BY PROBING THE DIE. THE UPPER LEFT INSET IS AN ENLARGED VIEW OF THE WIRE-BONDED DIE ON THE PRINTED CIRCUIT BOARD. THE LOWER LEFT INSET IS AN ENLARGED VIEW OF THE SILICON DIE (THE WHITE SQUARES ARE THE PADS USED FOR PROBING).

Phased arrays rely on the ability to accurately set the relative phases and amplitudes in the different signal branches. Errors and mismatches create non-idealities in the radiation pattern, such as beam pointing error and reduced directivity. This requires a system for quickly and accurately setting the phase and amplitude in each branch of a phased array. The possibility being explored is to employ dual feedback loops: the first operates on the phase of the output and generates the phase shifter control voltage, and the second operates on the amplitude of the output and generates the variable gain amplifier control voltage. The inputs to the system are the desired phase and amplitude, and the negative feedback action of the loops forces the control voltages to settle to their required values.

Phased arrays are primarily used for radar and other specialized applications, and often use discrete components or costly compound semiconductor technology. The possibility of implementing key components of a phased array in CMOS technology opens the door for the widespread adoption of phased arrays in communications applications. This research currently implements phase and amplitude control for a transmitter. The next step will integrate the system with the other transmitter components and then test the unit as a whole. EE

FACULTY ADVISOR: PROFESSOR DAVID J. ALLSTOT
COLLABORATORS: JAY RAJAGOPALAN
RESEARCH AREA: RADIO FREQUENCY INTEGRATED CIRCUIT DESIGN
GRANT/FUNDING SOURCE: INTEL CORPORATION

Self-Assembling Robots

SAM BURDEN, UNDERGRADUATE (EE)

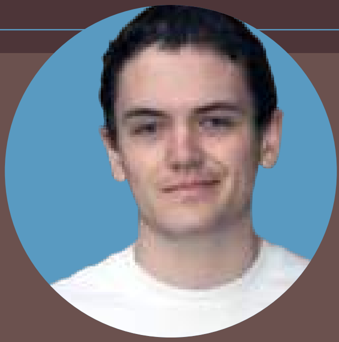

Self-assembly is a phenomenon that occurs in a variety of contexts in nature, motivating chemical reactions and cell metabolism. If one could engineer these types of processes, constructing an integrated circuit would be as simple as throwing a million tiny identical components in a beaker and gently shaking it. The Self-Organizing Systems Lab is studying the mathematical underpinnings of self-assembly. It seeks to direct disparate systems like DNA molecules and passive robots to organize in specified ways using similar formal models.

In an attempt to understand self-assembly in an extremely simple environment, a set of triangular robotic tiles that float on a frictionless air table has been constructed. These tiles are supposed to model molecules in a chemical reaction or proteins in a cell. Oscillating fans mix the tiles randomly and when the tiles collide, they latch. Once latched, the tiles can communicate with one another, decide whether or not to stay together, and either remain latched or break apart. By programming the tiles with different decision-making algorithms, a variety of final structures can be predictably produced.

Whether or not tiles interact and decide if they should stick together is analogous to macromolecules forming or breaking bonds and changing their internal structure when they interact with one another. By studying assembly processes involving these tiles, fundamentals about molecular self-assembly can be learned.

Progress has been made in determining efficient pathways for some assembly processes, which could be used to optimize the assembly of geometric structures like viral capsids. The goal of this research is to optimize assembly processes for these tiles and apply that information to other assembly contexts. EE

IMAGES SHOWING SIMULATED ROBOTIC TILES PROCEEDING FROM A DISCONNECTED STATE TO A FINAL TRIANGULAR ASSEMBLY.

FACULTY ADVISOR: PROFESSOR ERIC KLAVINS
RESEARCH AREA: SELF-ASSEMBLY
GRANT/FUNDING SOURCE: NSF

Markov Models to Perform Clinical Skills Assessment

THOMAS MACKEL, GRADUATE STUDENT (EE)

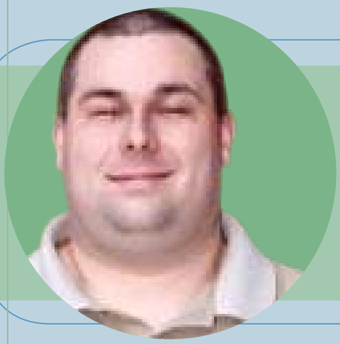

Inspired by an analogy between medical procedure and spoken language, Markov Models were used to classify subjects using the E-Pelvis simulator (Stanford) with 92% accuracy. Certain model aspects revealed information about the medical procedure's "grammar," which will help develop a more compact model representation and a generalized methodology.

Complicated medical procedures are a series of less complex sub-procedures, like "tying a knot," or "cutting tissue." These sub-procedures are a series of even more simple gestures, and gestures are a series of specific measurable forces. Forces (syllables), gestures (words), sub-procedures (sentences), and procedures (paragraphs) form the basis of the "language" of medical procedure.

Starting with force data obtained from experts performing an actual medical procedure, each continuous value data point is quantified to 1 of 32 discrete states, which are referred to as "syllables." This is analogous to each syllable having many different possible "pronunciations." A model of the expert data consists of the frequency of all expert syllable transitions, and the mean and covariance of the pronunciations associated with each syllable. A similar model is created from novice force data.

Force data taken from an unclassified subject is then used to make a third model, like the above two. Comparing the unclassified subject's model to the expert model yields an "Expert Skill Factor (ESF)," which represents how closely the subject's performance matched the performance of the aggregate of expert subjects. A Novice Skill Factor (NSF) is determined as well. Plotting the ESF vs. NSF shows a quantitative comparison of skill, referred to as the Performance Index, for multiple subjects.

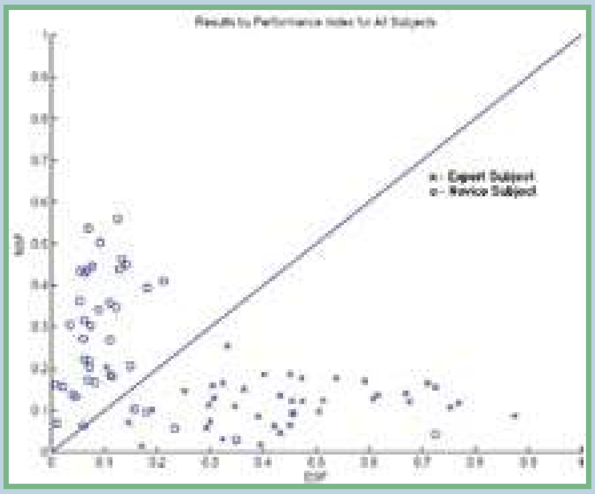

SKILL FACTOR PLOT SHOWING THE CLASSIFICATION RESULTS OF 82 SUBJECTS. THOSE ON THE TOP LEFT OF THE DECISION BOUNDARY ARE CLASSIFIED AS NOVICE, WHILE THOSE TO THE BOTTOM RIGHT ARE EXPERTS. THE ACTUAL SKILL LEVEL OF EACH SUBJECT IS REVEALED AFTER DETERMINING THE RESULT.

This skill assessment technique is heading towards handling larger dimensional data with many more syllables, as well as extending the number of classes beyond two. Another possible direction is to work on identifying "words" and "sentences" of the procedure, and using this information to simplify the models. EE

FACULTY ADVISOR: PROFESSOR JACOB ROSEN
COLLABORATORS: PROFESSOR BLAKE HANNAFORD (EE)
RESEARCH AREA: SURGERY
GRANT/FUNDING SOURCE: US ARMY MEDICAL RESEARCH AND MATERIEL COMMAND

Development of a 7 DOF Upper-Limb Exoskeleton

JOEL C. PERRY, LEVI M. MILLER, GRADUATE STUDENTS (ME)
BOBBY DAVIS, GRADUATE STUDENT (EE)

An exoskeleton is a wearable external robot with joints and links corresponding to those of the human body. Through the use of gravity compensation, the exoskeleton supports the weight of itself, the human arm, and externally applied loads while the human controls its motion through neural inputs using surface electromyography-based (sEMG-based) or impedance-based control algorithms.

As a proof of concept for neural control (sEMG), two prototypes of exoskeleton arms were developed. The first prototype produced a single-joint (elbow) exoskeleton controlled by sEMG signals from the bicep and tricep muscles. The second prototype included two additional degrees of freedom at the shoulder.

The current seven degree-of-freedom (DOF) exoskeleton, serving as a wearable robot, is composed of seven cable-driven aluminum links.

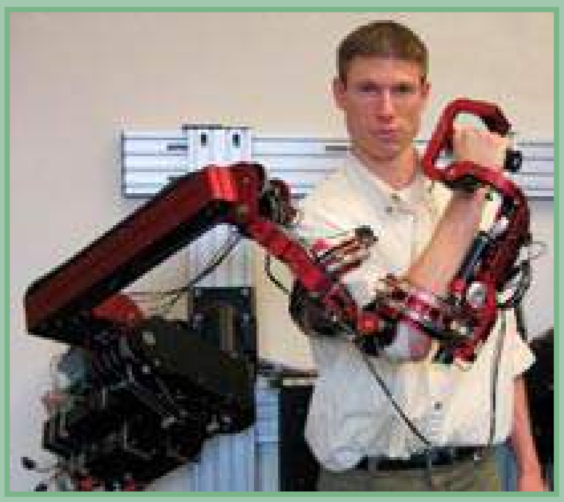

THE 7 DOF EXOSKELETON ARM IS CONNECTED TO THE USER AT THE THREE INTERFACE POINTS: THE HAND, FOREARM, AND UPPER ARM. INTERFACE CONTACT FORCES, JOINT POSITIONS, AND SEMG SIGNALS ARE USED TO CONTROL THE ROBOT AS A NATURAL EXTENSION OF THE OPERATOR'S ARM.

Complex pulley arrangements transmit torques from motor space to joint space. Shoulder and elbow transmissions are implemented with two-stage pulley reductions, while wrist joint transmissions use single-stage planetary gear reductions followed by single-stage pulley reductions. Proximal placement of motors effectively minimizes weight and inertia of moving segments whereas distal placement of pulley reductions maximizes transmission stiffness.

An underlying gravity compensation algorithm is used to cancel gravitational effects while a higher-level control law is used to calculate additional desired joint torques. Contrary to most gravity compensation implementations, no known position trajectory is fed to the controller, eliminating the possibility of correcting steady-state errors through feedback. As a wearable robot that is physically attached to the human body, the exoskeleton naturally follows the operator's command. Using a muscle modeling approach with myoprocessors as its core elements, the system predicts joint torques from sEMG signals while using an impedance control law.

Among the exoskeleton's potential applications, the proposed control strategy will enable persons with neuromuscular impairments to improve and potentially regain upper-limb function and mobility. Potential applications that will be further studied include rehabilitation and automatic physiotherapy, as well as using the exoskeleton as a haptic device while generating force feedback in virtual reality environments. EE

FACULTY ADVISOR: PROFESSOR JACOB ROSEN
COLLABORATORS: PROFESSOR BLAKE HANNAFORD (EE), DR. STEPHEN BURNS (REHAB. MED.)
RESEARCH AREA: CONTROLS AND ROBOTICS
GRANT/FUNDING SOURCE: NATIONAL SCIENCE FOUNDATION

Measurement of Grasper-Induced Tissue Damage

SMITA DE, GRADUATE STUDENT (BIOENG)

The use of minimally invasive surgical (MIS) techniques has greatly increased over the last couple of decades due to a number of patient benefits. However, limited force feedback in MIS tools (including surgical robots) may lead to inadvertent excess stress application by a surgeon and clinically significant tissue injury.

Reducing intra-operative or acute injury that can occur during routine tissue manipulation with surgical graspers may help to avoid unnecessary long-term consequences. Therefore, identification of relevant stress magnitudes and durations that can be safely applied to tissues may help improve MIS device design.

By measuring tissue damage as a function of stress magnitude and duration in commonly manipulated organs, safe stress "thresholds" can be identified and applied during minimally invasive surgery. The initial step to this project involved designing an appropriate methodology and analyzing it with preliminary studies. Combinations of experimental and analytical approaches were used to address these goals. Measured stresses, within the range of stresses typically applied with graspers by surgeons, are applied in vivo to pig liver, small bowel and ureter using the computer-controlled Motorized Endoscopic Grasper (MEG) developed in the UW Biorobotics Laboratory.

Histological methods and image analysis are used to measure acute injury in the compressed tissues based on inflammation, coagulation and cellular death. Finite element modeling is used to approximate stress distributions under the MEG's grasper jaws for a more accurate correlation of stress to tissue damage.

Multiple models will be created for each organ, with a stepwise increase in model complexity. Statistical analysis, including analysis of variance, is used to identify stress magnitudes and durations that cause significantly increased acute damage to organs.

Initial results indicate an appropriately sensitive methodology. Preliminary results produced expected finite element models and nonlinear relationships between stress and damage, suggesting that it may be possible to identify safe stress thresholds. EE

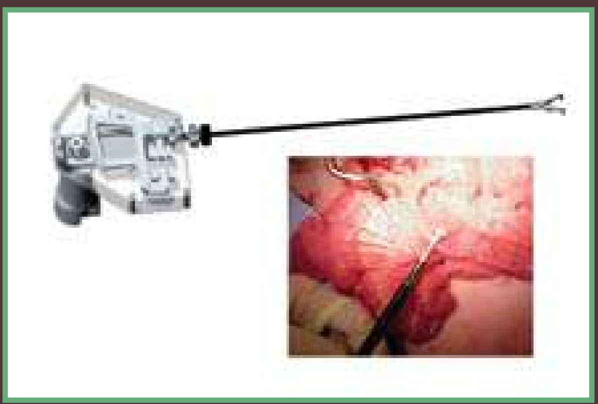

CAD DRAWING OF THE MEG. INSET SHOWS PHOTOGRAPH OF THE MEG GRASPING SMALL BOWEL DURING AN IN VIVO EXPERIMENT.

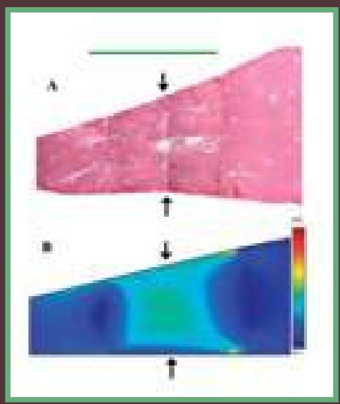

A) H&E STAINED SECTION OF IN VIVO LIVER WITH A VERTICAL COMPRESSION OF 197 KPA. GREEN BAR=WIDTH OF GRASPER JAWS. B) 2D STATIC FEM WITH PROPERTIES OF LIVER AND A 200 KPA VERTICAL STRESS, SIMILAR TO A (MAGNITUDE SCALE IS ON RIGHT). NOTE VARIED STRESS DISTRIBUTION APPROXIMATED BY FEM AND CORRELATION OF VASCULAR DAMAGE (BLEEDING) TO STRESS CONCENTRATIONS IN THE LIVER SECTION (A).

FACULTY ADVISOR: PROFESSOR BLAKE HANNAFORD
COLLABORATORS: PROFESSORS MIKA SINANAN (SURGERY), PAUL SWANSON (PATHOLOGY), JACOB ROSEN (EE) AND GEORGE TURKIYYAH (CIVIL ENG)
RESEARCH AREA: MINIMALLY INVASIVE SURGERY
GRANT/FUNDING SOURCE: NSF, ARMY, CENTER FOR VIDEOENDOSCOPIC SURGERY, DEPARTMENT OF ANATOMIC PATHOLOGY

Haptics in a Shared Virtual Environment

GANESH SANKARANARAYANAN, GRADUATE STUDENT (EE)

Haptic systems provide a sense of touch as feedback signal for the operator of a device. The device might be physical, such as a remotely operated robot, or a virtual object. When there are two or more operators in a networked haptic environment, maintaining position coherency between the copies of the virtual object is necessary to achieve consistency in collaboration. This is especially important in the presence of time delays. Three virtual coupling schemes were introduced in this work to maintain position coherency. Experimental results demonstrate their effectiveness.

It has been shown that the inclusion of haptics in a shared virtual environment increases the task performance and virtual presence felt by the users. Previous work in this area includes systems with impulsive force rendering and haptic media synchronization techniques such as intra-media, inter-media and group synchronization control.

The collaborative haptic control of a two-user, one degree of freedom, simplified collaboration setup is explored in this work. The experimental setup consists of a cube that is free to move along one degree of freedom on a floor inside a three dimensional room rendered using OpenGL. A similar virtual environment was displayed for the second user on a separate computer. The display also includes a target sphere that both users jointly track during the experiment. Two PHANToM Omni haptic devices were used to interact with the cube. Three different virtual coupling schemes for position coherency were wasted: distributed architecture (Scheme 1), peer-to-peer architecture (Scheme 2), and a centralized or client-server architecture (Scheme 3).

The performance of all three approaches was evaluated experimentally, using ten volunteers. A fixed set of virtual coupling parameters was used. Position coherence in terms of peak and RMS position error between the two cubes was computed for each method. As expected, the centralized architecture had the lowest position error. The distributed architecture resulted in a position error only slightly higher than the centralized architecture, for the delays that were tested in this work. The peer-to-peer method had substantially higher position errors.

It has been demonstrated that a distributed control architecture can achieve a comparable performance to that of a client-server approach. Networks like the Internet have time-varying delay, and communication packets could be lost or arrive out of order. The next step is to investigate this.EE

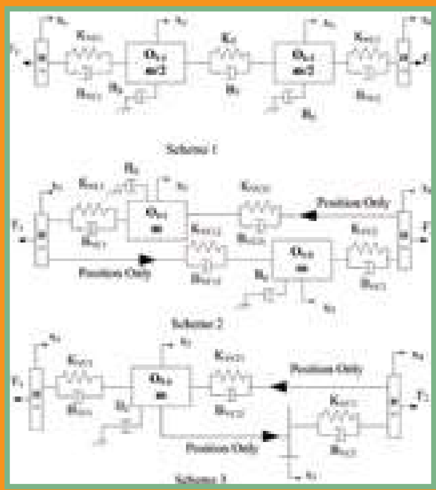

THIS FIGURE SHOWS THE THREE VIRTUAL COUPLING SCHEMES. SCHEMES 1 AND 2 ARE PEER-TO-PEER ARCHITECTURE, AND SCHEME 3 IS CLIENT-SERVER ARCHITECTURE.

THE RMS POSITION ERROR BETWEEN THE TWO CUBES. SCHEME 1 HAS A COMPARABLE PERFORMANCE TO SCHEME 3 FOR DELAYS UP TO 200 MS.

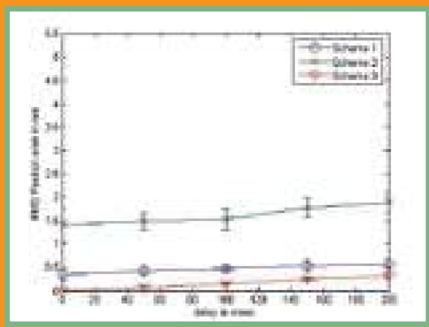

GANESH SANKARANARAYANAN AND SMITA DE, GRADUATE STUDENTS AT THE BIOROBOTICS LABORATORY ARE COLLABORATING USING THE EXPERIMENTAL SETUP.

FACULTY ADVISOR: PROFESSOR BLAKE HANNAFORD
COLLABORATORS: STEVEN VENEMA, JIM TROY AND KEVIN PUTERBAUGH – BOEING
RESEARCH AREA: COLLABORATIVE HAPTICS, TELEOPERATION
GRANT/FUNDING SOURCE: BOEING

Next Generation Robotic-Assisted Surgery

MITCHELL LUM, KENNETH J. FODERO II, H. HAWKEYE I. KING,
GANESH SANKARANARAYANAN, GRADUATE STUDENTS (EE)
DENNY TRIMBLE, GRADUATE STUDENT (ME)
GINA DONLIN, CLINT BLAND, UNDERGRADUATES

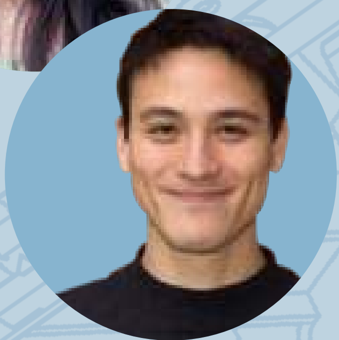

Surgical robotics will revolutionize the way in which surgical intervention is performed. The integration of robotics and medicine will ultimately lead to better patient care. Less invasive procedures, more precise motion control, and quicker healing times are just a few of the potential benefits.

The first generation of surgical robots made a significant step toward integrating robotics and medicine. However, some of these systems were large and overbuilt. The BioRobotics Lab (BRL) is working on the next generation in surgical robotics. Primary electronics and a mechanism optimized for the requirements of minimally invasive surgical (MIS) procedures are in place. The BRL is currently working on control software, teleoperative control design, and user interfaces for local and remote control. As the field of surgical robotics continues to evolve, it is important to keep patient safety in mind. A safety control architecture is being developed that is aimed at moving an experimental system in the direction of intrinsically safe operation.

This project is part of the “operating room of the future” vision in which the patient is the only person in the room and doctors teleoperate robotic manipulators to perform surgery. The BRL Surgical Robot is being developed by an interdisciplinary team with members from the departments of surgery, electrical engineering, mechanical engineering, bioengineering and computer science. This surgical robot, which is currently a prototype undergoing testing, is composed of a number of subsystems. It is a two arm, 7-DOF, cable-actuated surgical robot system for performing minimally invasive telesurgery. Using a multidisciplinary approach to design the system will lead to a seamless integration into the operating room of the future.

MIS utilizes long slender tools and a video camera inserted through ports in the patient. Operating about this pivot point makes a spherical mechanism a natural candidate for a MIS robot manipulator. Using in-vivo MIS kinematic and dynamic data as a foundation, an optimization was performed to determine the ideal link angles for the 2-R spherical linkage. The dexterous workspace (DWS) is defined as the workspace in which surgeons spend 95% of their time, and the extended dexterous workspace (EDWS) as the workspace required to reach all the target anatomy in the human abdomen. Kinematic analysis of the 2-R spherical mechanism led to the derivation of the forward and inverse kinematics as well as the Jacobian matrix.

Isotropy is a measure of how well a manipulator can move in any arbitrary direction and is defined as the ratio of highest to lowest singular value of the Jacobian matrix. This score is unbounded, so isotropy is redefined as the ratio of the lowest to highest singular value to obtain a bounded scoring criterion that ranges from 0 (singular) to 1 (perfectly isotropic). There is an isotropy score associated with every pose of every design.

In order to perform an optimization over the design space, all combinations of link angles ranging from 16°-90° were analyzed with respect to isotropy. For each potential target workspace, the isotropy score is integrated over the workspace then multiplied by the minimum score within that target workspace. This provides a measure of average performance as well as penalizing target workspaces near singularities. The best target workspace score for each design candidate is then divided by the sum of the link angles cubed to provide a penalty for greater mass and inertia. The optimal manipulator is defined as the design of the highest composite score when scored against the DWS, but can also reach the entire EDWS. The resulting design for a 2-R spherical mechanism optimized for MIS yielded link angles of 75° and 60° (Link1 and Link2 respectively). These parameters were the basis for the mechanical design work required to bring this system to fruition.

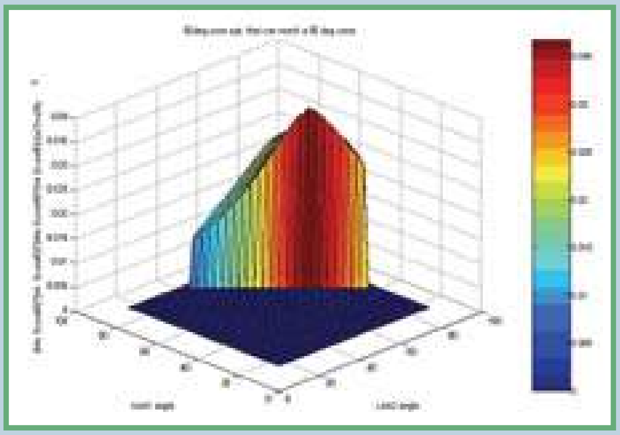

DESIGN SPACE SCORE AS A FUNCTION OF LINK ANGLES.

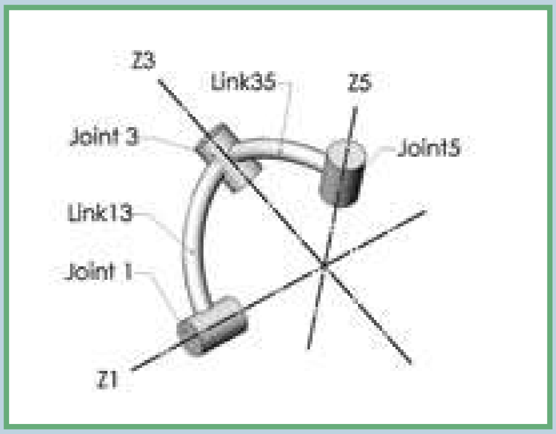

SPHERICAL MANIPULATOR, LINK AND FRAME ASSIGNMENTS.

The first four joint axes of the robot intersect at the surgical port location resulting in a spherical motion about the incision point that allows for tool motion just as in manual MIS. DC brushless motors mounted to the base of the surgical manipulator actuate all motion axes. Maxon EC-40 motors with 12:1 planetary gearboxes are used for the first three axes, which see the highest forces. Maxon EC-32 motors are used for the remaining axes. Maxon DES70/10 series amplifiers drive these brushless motors. The motors are mounted on quick-change plates, allowing for motor removal without the need for disassembling the cable system. The first three axes have power-off brakes to prevent tool motion in the event of a power failure.

THE BRL 7-DOF SURGICAL MANIPULATOR IS A CABLE-ACTUATED SYSTEM WITH ALL OF THE BRUSHLESS ACTUATORS MOUNTED ON ITS BASE. LINKS WERE OPTIMIZED BASED ON IN-VIVO MIS DATA COLLECTED ON PORINCE MODELS AS WELL AS HUMAN MEASUREMENT. THE COMPLETE SYSTEM INCLUDES TWO ARMS, WITH THE CONTROL SOFTWARE RUNNING ON AN RTAI LINUX COMPUTER.

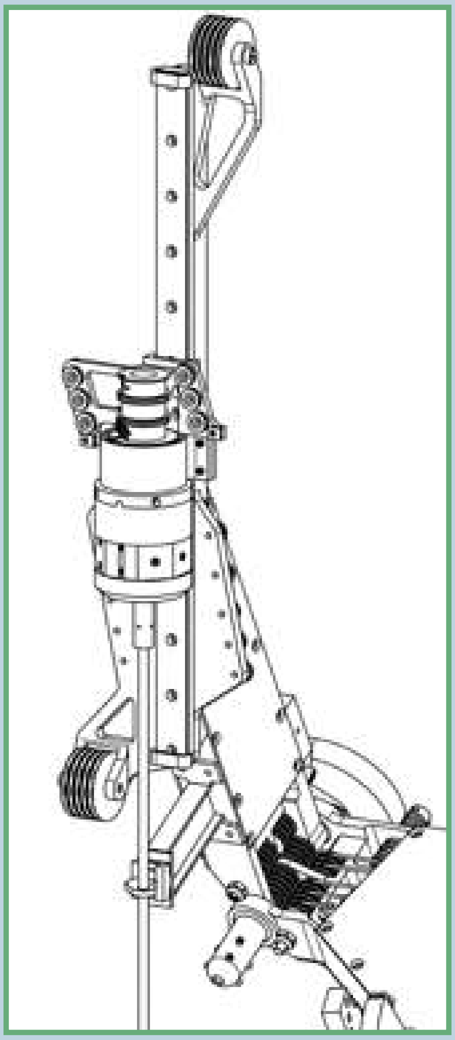

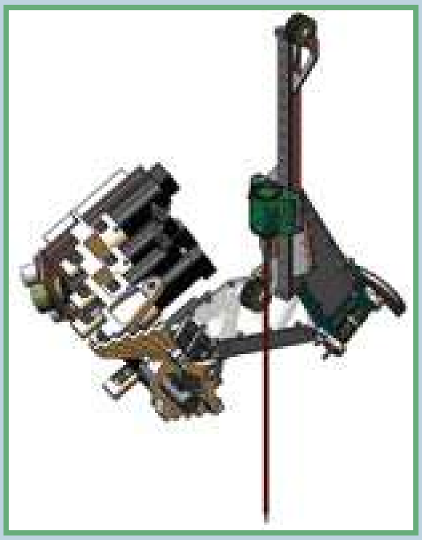

A CAD SHADED IMAGE OF THE SURGICAL ROBOT. CABLE ACTUATED WITH MOTORS ARE MOUNTED ON A STATIC BASE. THE COMPLETE SYSTEM WILL FEATURE TWO MIRROR IMAGE DESIGNED ARMS, ONE FOR EACH OF THE SURGEONS HANDS, PLUS A CAMERA HOLDING/POSITIONING ROBOT.

A CAD LINE DRAWING OF THE SECOND LINK AND TOOL INTERFACE BOX OF THE SURGICAL ROBOT. THE TOOL INTERFACE FEATURES QUICK RELEASE TOOLS THAT SUPPORT BEING INTERCHANGED DURING SURGERY BY A 'SCRUB NURSE ROBOT' TOOL CHANGER.

The control software is running on Linux with real-time extensions to the kernel (RTAI). The controller is implemented as a kernel module and RTAI grants it exclusive access to system resources, turning a full-featured application on Linux into an embedded-type system with highly accurate timing. The robot control loop runs at 1kHz.

Well-defined software interfaces to the controller allow high-level control of the robot (start, stop, control gains, test inputs, etc) from the Linux host and surgical control by a master device across a network. The master device can be any suitable, high fidelity haptic interface; currently the Phantom Omni from Sensable Technologies is used. The surgeon interface also uses touch screen controls and foot pedal for user-friendly operation during surgery.

Connection between the robot and the Linux host is through a USB 2.0 I/O board also developed in the BRL. Custom drivers allow the board to communicate with RTAI Linux in USB 2.0 bulk transfer mode. This USB board is designed to be highly versatile and includes a variety of inputs and outputs, including 8 24-Bit Encoders, 8 16-Bit DACs and 8 General Purpose I/O Pins. PC control software can set DAC values output to the DES 70/10s controlling motor torques, or read encoder values to get the robot joint positions.

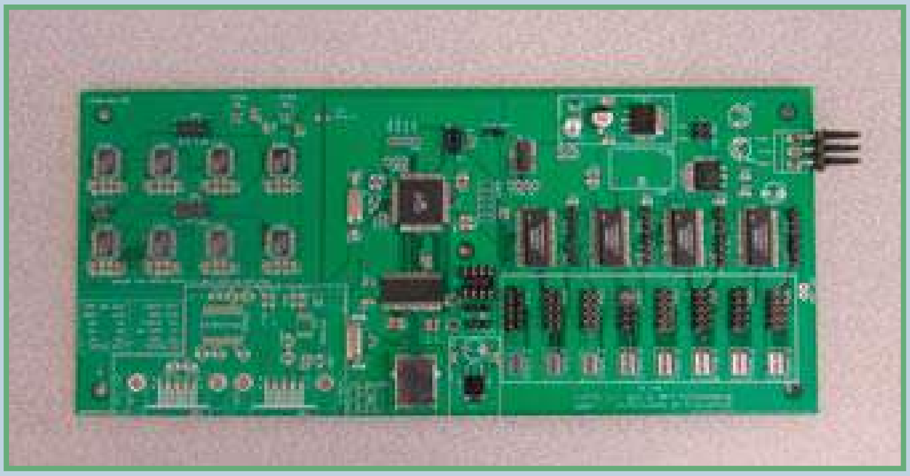

THE FULLY ASSEMBLED USB INTERFACE BOARD.

This surgical robot will have a variety of safety features. These features include a small number of operating states, brakes, an emergency stop (E-Stop) button, a watchdog timer, and a surgeon side foot pedal. The state of the system will be managed by a programmable logic controller (PLC). PLCs are a highly reliable off the shelf technology that can easily be programmed for small numbers of states. The control software will send requests to change states to the PLC and the PLC will in turn update the states. Additionally, a function in the Control Module produces a 10Hz square wave for a watchdog timer function in the PLC.

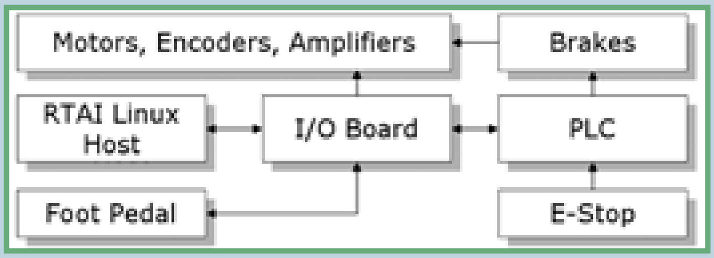

THE SYSTEM SOFTWARE IS MODULAR, AND ALLOCATION OF SOFTWARE MODULES TO COMPUTING HARDWARE IS FLEXIBLE EXCEPT FOR THE I/O BOARD SOFTWARE AND THE PLC LADDER LOGIC.

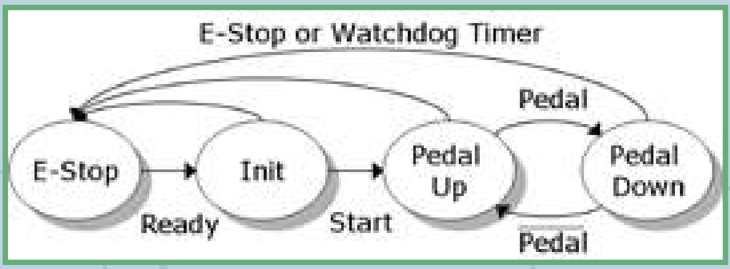

THE SYSTEM WAS DESIGNED TO CONSIST OF FEW STATES, AS SHOWN IN THIS FIGURE. MOVEMENT BETWEEN THESE STATES OCCURS DUE TO SIGNALS SENT INTO THE PLC. TRANSITIONS BETWEEN PEDAL UP AND PEDAL DOWN ARE CONTROLLED BY SURGEON FOOT PEDAL.

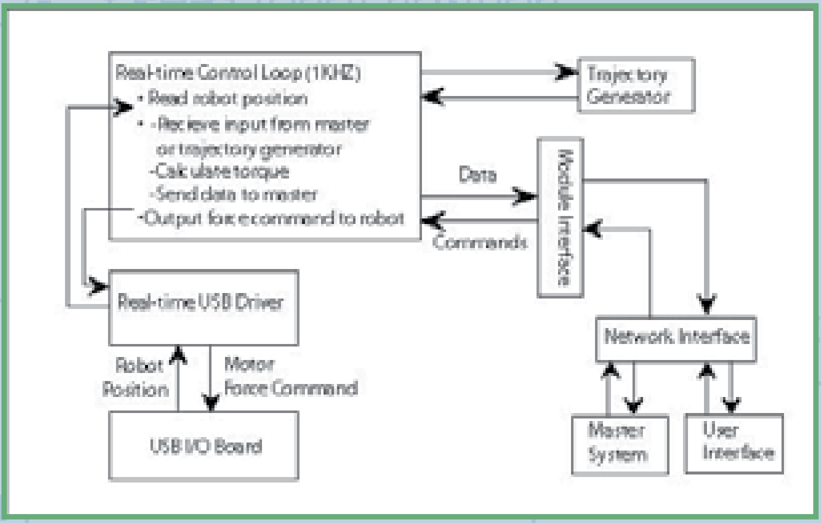

A BLOCK DIAGRAM SHOWING THE MAJOR CONTROL SYSTEM COMPONENTS. CONTROL SYSTEM RESIDES ON A LINUX HOST WITH REAL-TIME (RTAI) EXTENSIONS.

The design of this safety system is almost complete. The process of testing and constructing the various pieces of the system has begun, and the hope is to have the safety system constructed soon. The described software architecture is a crucial element in the overall surgical robot system. The expectation is that this system will provide a level of predictability, reliability and robustness sufficient for animal surgery evaluation.

Another aspect of this project is teleoperative control and mediating the destabilizing effects of time delay. A low-latency network protocol stack for RTAI decreases network latency, but cannot nullify the large and variable time-delays associated with operating across the Internet.

The researchers in the BRL are testing, applying and advancing the state of the art technology in this field. The system successfully performed a teleoperation demonstration across the UW campus from Kane Hall to the BioRobotics Lab with the first three DOF under control. This highly portable, network-enabled surgical platform has the potential to bring the skill of expert surgeons anywhere in the world.EE

FACULTY ADVISOSR: PROFESSORS BLAKE HANNAFORD AND JACOB ROSEN
COLLABORATORS: PROFESSOR MIKA SINANAN - CENTER FOR VIDEO ENDOSCOPIC SURGERY (DEPT. OF SURGERY)
RESEARCH AREA: CONTROLS AND ROBOTICS, SURGICAL ROBOTICS, CONTROLS, TELEOPERATION
GRANT/FUNDING SOURCE: US ARMY – MEDICAL RESEARCH AND MATERIAL COMMAND GRANT NUMBER: DAMD-17-1-0202;\

Automated Single-Cell Analysis

JOHN KOSCHWANEZ, GRADUATE STUDENT (EE)

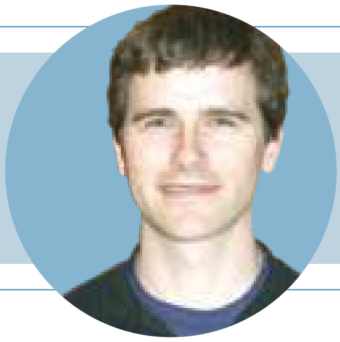

Why do we age? How do we age? Science still cannot answer these fundamental questions, yet we know that a cell's genome becomes unstable over time—understanding why this occurs could lead to treatments for age-related ailments such as cancer.

Yeast cells are an ideal model organism for studying human aging, but analyzing old yeast cells is extremely labor intensive. This research combines the fields of automation, electromagnetics, image processing, microfluidics and cellular biology to develop a system that will automate the lifetime analysis of a single yeast cell.

This automated system will be used to determine what causes age-related genomic instability. Yeast culture is pumped into a microfluidic device, where a single yeast cell is captured by microfabricated magnets. This yeast cell is held for its lifetime, which is approximately 60 hours. Image processing software is then used to monitor the cell and automatically detect the cell dividing into a mother and a daughter cell. When the cell divides, valves in the microfluidic device align to send the daughter cell to an external petri dish, where it is grown for future genetic analysis. Each daughter colony gives a snapshot of the genetic stability of the mother at the time of the division.

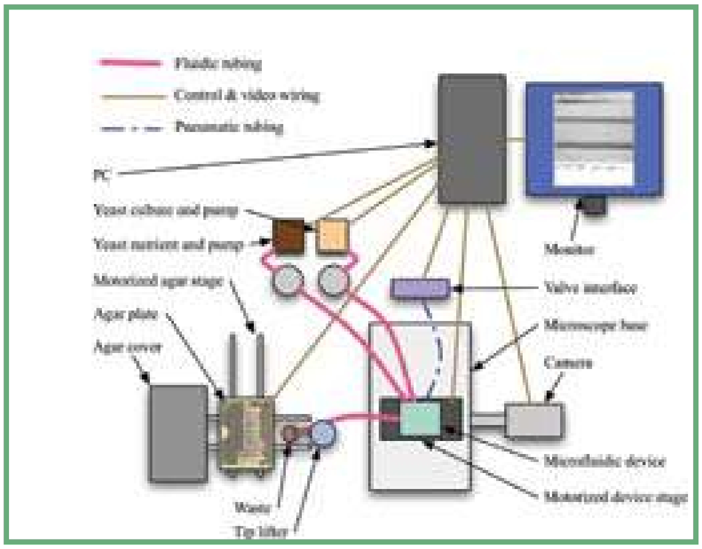

A SCHEMATIC OF THE AUTOMATED YEAST LIFETIME ANALYSIS SYSTEM. YEAST CELLS ARE CAPTURED IN THE MICROFLUIDIC DEVICE, WHERE THEY ARE MONITORED BY THE COMPUTER. DAUGHTER CELLS ARE DEPOSITED ON AN AGAR PLATE WHERE THEY ARE STORED UNDER A STERILE COVER FOR GENETIC ANALYSIS.

After the system has been tested for a single cell, it will be expanded to monitor the lifetimes of 100 cells in parallel. This will allow the experiment to be run under the different environmental conditions and genetic backgrounds required to elucidate the mechanism of age-related genomic instability. Eventually, the system will automate a wide variety of aging analyses in yeast and human cells. EE

FACULTY ADVISOR: PROFESSOR DEIRDRE R. MELDRUM
COLLABORATORS: DANIEL GOTTSCHLING (FRED HUTCHINSON), ROBERT CARLSON (EE), PROFESSOR MARK HOLL (EE)
RESEARCH AREA: BIOLOGICAL INSTRUMENTATION
GRANT/FUNDING SOURCE: NIH NHGRI

Confocal Microscopy

JOSEPH CHAO, RESEARCH ASSOCIATE (EE)

Fluorescence imaging has become an important tool for studying dynamic gene expression and protein functions. Confocal microscopy is especially gaining popularity due to its three-dimensional capability, which enables biologists to study cellular responses.

However, the availability of information and the accessibility of new ideas in medical and biological research often requires expensive instruments and labor-intensive operations. For example, commercial confocal microscopes are a powerful tool for life sciences and nanotechnology, but they are expensive, large in size, and limited in function.

The Microscale Life Sciences Center (MLSC) is utilizing new technologies to make confocal microscopes smaller, less expensive and able to modulate light in temporal and spatial domains. As a result, these new microscopes with lab-on-a-chip devices can observe biological events that cannot be seen by conventional means. Furthermore, the size and cost of the system are comparable to a digital projector, making confocal microscopy affordable for more laboratories and individuals.

A MICROGRAPH OF A LIVING CELL ARRAY AT THE MLSC USING THE DIGITAL CONFOCAL MICROSCOPE. THE MICROSCOPE CONTROLS LIGHT PROJECTED TO FIVE CIRCULAR MICROCHAMBERS THAT WILL HOUSE CELLS OF INTEREST.

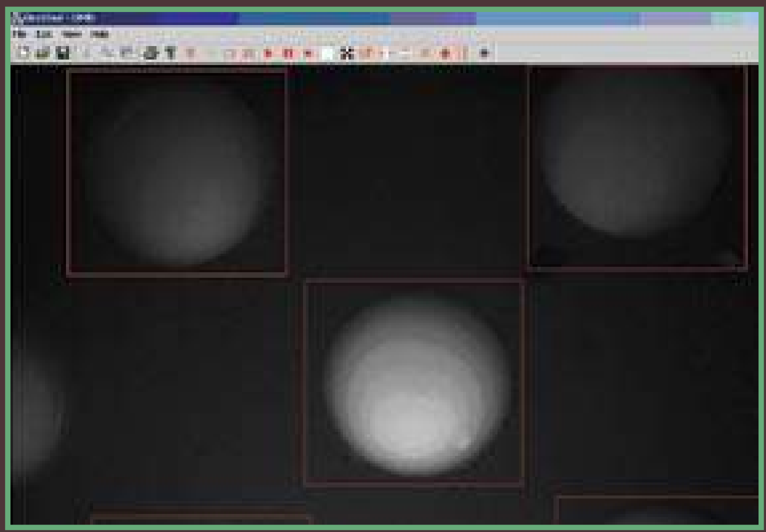

The new system will be used with the high-content living cell array developed at MLSC, (co-directed by EE Professor Deirdre Meldrum and Microbiology and Chemical Engineering Professor Mary Lidstrom) to monitor dynamic multi-variable cellular processes. EE

FACULTY ADVISOR: PROFESSOR DEIRDRE R. MELDRUM
RESEARCH AREA: BIO-INSTRUMENTATION
GRANT/FUNDING SOURCE: NIH

Single-Cell Trapping Using Fluid Tweezers

BARRY R. LUTZ, RESEARCH ASSOCIATE (EE)

Though genome sequencing has provided instructions for life, cells with identical genes show a range of behaviors due to randomness in translating these instructions. Insight into these variations will require innovative tools for manipulating individual cells under conditions that mimic their natural environment.

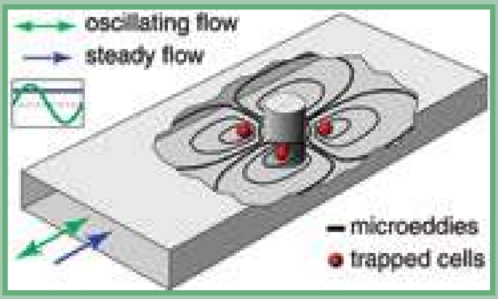

A SCHEMATIC REPRESENTATION OF A TRAPPING DEVICE. A PORTION OF THE CHANNEL WALL IS REMOVED TO SHOW THE CHANNEL INTERIOR. FLUID OSCILLATIONS (AC, GREEN) CREATE FOUR SYMMETRIC MICROEDDIES AROUND A CYLINDER (BLACK CONTOURS), WHILE SUPERIMPOSED STEADY FLOW (DC, BLUE) LEADS TO ASYMMETRIC EDDIES (NOT SHOWN). EACH MICROEDDY SUSPENDS A SINGLE CELL (RED) IN THE FLUID AWAY FROM SOLID SURFACES.

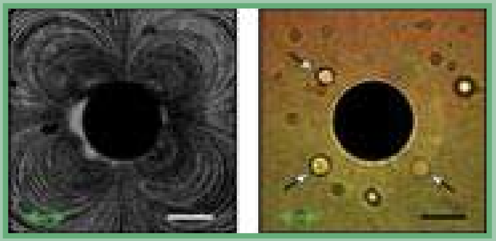

EXPERIMENTAL IMAGES OF MICROEDDIES AND TRAPPED CELLS IN AC FLOW (GREEN ARROWS). LEFT – TRACER PARTICLES SHOW THE FLOW OF FOUR SYMMETRIC EDDIES AROUND A CYLINDER. RIGHT – MICROEDDIES SUSPEND HUMAN T-CELLS (WHITE-HEADED ARROWS) IN A GENTLE FLOW. SCALE BARS 50 MICRONS.

"Microfluidic" devices with tiny fluid channels offer exciting alternatives to conventional tools (e.g., flasks, pipettes) for studying cells in controlled chemical environments. However, it requires a method of positioning and holding cells in place without damaging them or affecting their behavior. This is especially difficult for cells that respond to the sense of touch. As a result, an unusual fluid flow to gently trap single cells in a microscopic channel has been developed.

A tiny cylinder, about the size of a human hair (100 microns), creates four microeddies when the fluid is oscillated (AC) at audible frequency. Each microeddy positions and holds a single cell near the eddy center, somewhat like a pop bottle trapped in a whirlpool.

Forces generated by the flow push inward from all directions to completely suspend a cell within the fluid. Trapping forces are comparable to well-known methods that use focused lasers (optical tweezers) or oscillating electric fields (dielectrophoresis). Because the gentle flow around the microeddies is comparable to blood flow in arteries, fluid tweezers provide a more natural environment for studying suspended cells.

A complete picture of cell-to-cell variation will require measurement of many single cells under controlled chemical conditions. Many traps are created in a single device using cylinder arrays, and cells are loaded into the traps by superimposing a steady flow (DC) on the oscillation.

The DC flow is also used to supply trapped cells with nutrients, reagents, and fluorescent indicators needed for dynamic measurements. Fluid tweezer arrays dosed with chemicals will be used to measure dynamic protein expression by human T-cells under physiological conditions.

The remarkable ability to suspend cells in a gentle fluid flow makes fluid tweezers well-suited for studying sensitive cells, such as human T-cells that normally live suspended in blood. EE

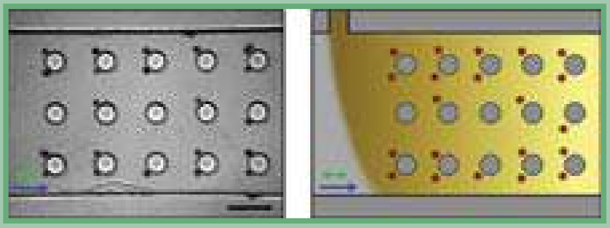

A TRAPPING ARRAY IMAGE AND SCHEMATIC OF CHEMICAL DOSING IN ARRAYS UNDER AC AND DC FLOW (GREEN AND BLUE ARROWS, RESPECTIVELY). LEFT – MICROEDDIES CREATED IN CYLINDER ARRAYS SHOW THE SAME ABILITY TO TRAP. SCALE BAR 200 MICRONS. RIGHT – THE DC FLOW DELIVERS NUTRIENTS AND OTHER CHEMICALS TO CELLS FOR DYNAMIC MEASUREMENTS.

FACULTY ADVISOR: PROFESSOR DEIRDRE R. MELDRUM
COLLABORATORS: PROFESSORS DANIEL T. SCHWARTZ AND JIAN CHEN (ChemE)
RESEARCH AREA: MICROFLUIDIC TOOLS FOR SINGLE-CELL ANALYSIS
GRANT/FUNDING SOURCE: NIH MICROSCALE LIFE SCIENCES CENTER (MELDRUM, PI), UW GENOME SCIENCES TRAINING GRANT (MELDRUM), BOEING-SUTTER ENDOWMENT FOR EXCELLENCE IN ENGINEERING (SCHWARTZ)

Opto-Plasmonic Tweezers

XIAOYU MIAO, GRADUATE STUDENT (EE)

The ability to control the orientation of biological cells is a particularly desirable manipulation mechanism. Such capability opens the door for building structured biomaterials with potential applications in constructing biofilms and human tissue engineering.

Recently, achieving such a goal using light has attracted much attention since the location of the exerted force can be not only precisely defined, but also flexible and controlled by scanning the light.

This research aims to design and build the Opto-Plasmonic Tweezers for manipulation and rotation of micro/nano objects.

Micro/nano objects with asymmetrical shapes are suspended in a liquid solution. The light source, with its polarization adjusted by a fine polarization controller, has an electric-field component and is focused on an Au-nanoshell film.

A simulated 3-D trapping trajectory with equal time interval for the micro/nano object which is trapped at the surface of the Au-nanoshell film.

This electric field oscillates in time with the frequency of the incident light, and induces the free electrons near the surface of the metal to move and form oscillating dipole moments. With the proper frequency, resonant oscillation can be induced, and surface plasmon is formed. The direction of the dipoles is parallel to the electric-field polarization of the light. They radiate in the same way as oscillating charges, and create a patterned radiation electric field that manipulates the micro/nano objects through dielectrophoresis with fine orientation control by adjusting the polarization of the incident light.

By developing a theoretical model, dielectrophoresis force and torque for asymmetrical objects can be analyzed. Using the self-assembled polystyrene monolayer as the template, an Au-nanoshell film was fabricated, which can be utilized to generate the surface plasmon resonance. In collaboration with Professor Suzie Pun from the UW Department of Bioengineering, a bench-top optical system using Listeria monocytogenes for the experimental demonstration will eventually be built.EE

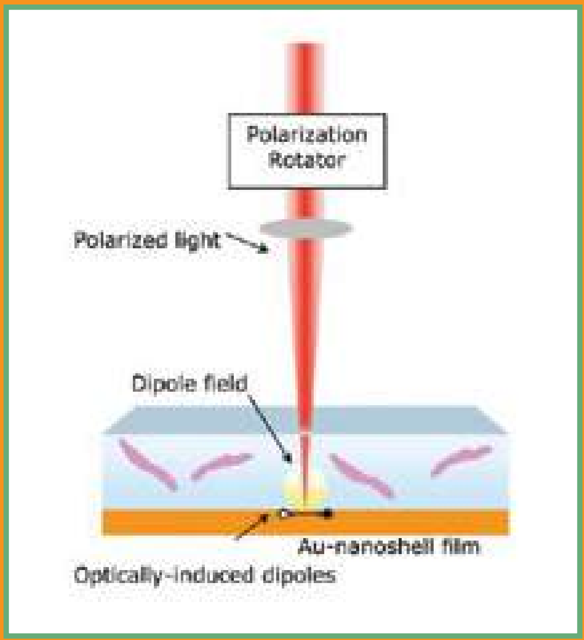

AN ILLUSTRATION DEPICTING THE MANIPULATION OF MICRO/NANO OBJECTS WITH ITS ORIENTATION CONTROLLED BY POLARIZED LIGHT.

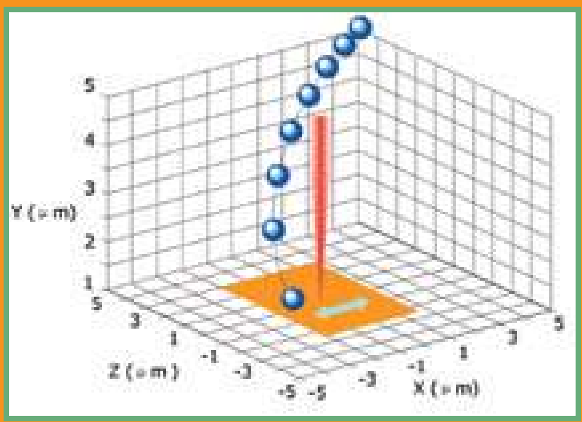

A SIMULATED 3-D TRAPPING TRAJECTORY WITH EQUAL TIME INTERVAL FOR THE MICRO/NANO OBJECT WHICH IS TRAPPED AT THE SURFACE OF THE AU-NANOSHELL FILM.

FACULTY ADVISOR: PROFESSOR LIH Y. LIN
COLLABORATORS: PROFESSOR SUZIE PUN (BIOENG)
RESEARCH AREA: BIOPHOTONICS
GRANT/FUNDING SOURCE: NSF & NIH

Nanophotonic Waveguides Using Self-assembled Quantum Dots

JEAN WANG, GRADUATE STUDENT (EE)

The diffraction limit stemming from Heisenberg's Uncertainty Principle limits the packing density of photonic components. Proposed methods are subject to difficulties in fabrication, integration with other photonic components and transmission loss. However, the quantum dot (QD) based nanophotonic waveguide is gain-enabled and may be constructed through self-assembly.

Working in the area of nanophotonics, this research involves guiding light at sub-diffraction limit dimensions. Both 500 nm and 100 nm width waveguides made by self-assembly of quantum dots on a substrate via an e-beam lithography template have been succesfully demonstrated.

The waveguide operation relies on a pump light to create population inversion within the quantum dots and a signal light to cause stimulated emission of photons, which allows the propagation of light through near-field energy transfer.

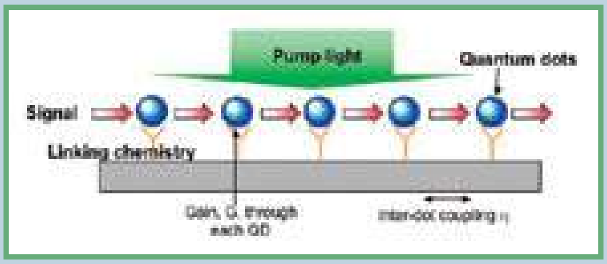

A QUANTUM DOT WAVEGUIDE OPERATION.

FLUORESCENCE PATTERNS OF 500 NM AND 100 NM WIDE WAVEGUIDES. (A) 500 NM WIDE WAVEGUIDE: I) SINGLE; TWO ADJACENT WAVEGUIDES SPACED II) 200 NM APART AND III) 500 NM APART. (B) 100 NM WIDE WAVEGUIDE – THE RESOLUTION IS DIFFRACTION LIMITED: I) SINGLE; TWO ADJACENT WAVEGUIDES SPACED II) 200 NM APART AND III) 500 NM APART.

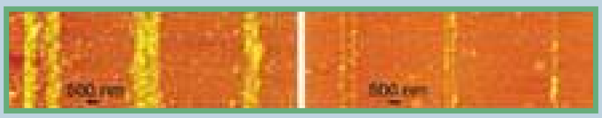

CORRESPONDING AFM IMAGES OF (A) 500 NM AND (B) 100 NM WIDE WAVEGUIDES IN SINGLE AND PAIRED FORMATION SPACED AT 200 NM AND 500 NM APART.

To place the quantum dots, fabrication begins by using e-beam lithography on a silicon dioxide coated silicon substrate to specify waveguide widths at 100 nm and 500 nm. Then, the samples are immersed in 3'aminopropyltriethoxysilane (APTES) followed by solution deposition of carboxylated QDs, where the carboxyl and amine group binding is facilitated by 1-ethyl-3-(3 dimethylaminopropyl)-carbodiimide (EDC).

The small number of steps involved enables rapid processing and placement of quantum dots at high density. Deposition of the first monolayer composed of APTES has been confirmed with x-ray photoelectron spectroscopy (XPS), which reveals up to 10 nm of the surface composition by element. In addition, fluorescence micrographs and AFM images, confirm the attachment of 655 nm emission quantum dots aligned in the 500 nm and diffraction-limited 100 nm width lines.

The next steps will test the waveguides by measuring loss, cornering efficiencies, and crosstalk between adjacent structures. The use of alignment marks and tapered patterns will aid in characterizing 100 nm waveguides. With thorough demonstration, quantum dot waveguides may become a useful mean for transporting information on the nanoscale. EE

FACULTY ADVISOR: PROFESSOR LIH Y. LIN
COLLABORATORS: PROFESSOR BABAK A. PARVIZ (EE)
RESEARCH AREA: ECDT - PHOTONICS
GRANT/FUNDING SOURCE: NSF GRADUATE FELLOWSHIP

Nano-Scale Quantum Dot Photodector

MICHAEL HEGG, GRADUATE STUDENT (EE)

The emerging field of nano-photonics offers the possibility of large bandwidth, high-speed, and high-density photonic integrated circuits for future use in all-optical computing and communications. Nano-scale, super-sensitive, single-photon detection devices will be a critical component of such circuits. The unique optoelectronic properties of quantum dots make these tiny pieces of semiconductor material well-suited for such an application.

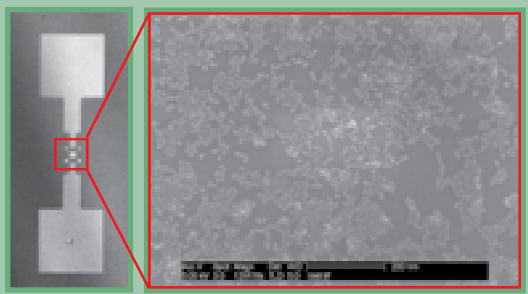

FLUORESCENCE (LEFT) AND SEM (RIGHT) MICROGRAPHS OF ELECTRODE STRUCTURE WITH QUANTUM DOTS SELF-ASSEMBLED IN BETWEEN.

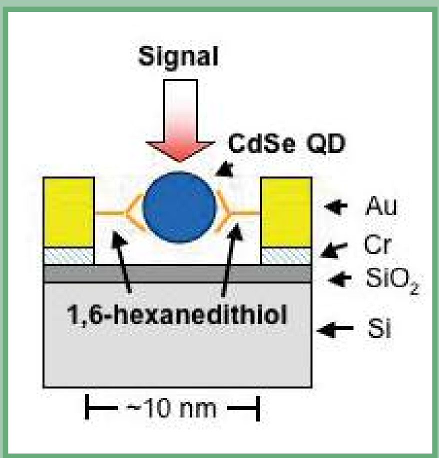

CONCEPTUAL GRAPHIC OF A NANO-SCALE QUANTUM DOT PHOTODETECTOR THAT SHOWS THE CDSE QUANTUM DOT LINKED TO THE AU ELECTRODE VIA THE HDT MOLECULE.

The photodetector described here consists of one or more quantum dots that bridge a small gap (~1 nm) between Au electrodes on a Si/SiO_2 substrate. The quantum dots are linked to the electrodes via a self-assembly process using hexanedithiol (HDT) as the linker molecule.

The Au electrodes are defined on the Si/SiO_2 substrate using electron-beam lithography (EBL). A monolayer of HDT is self-assembled on to the Au electrodes and CdSe quantum dots are subsequently self-assembled to the HDT monolayer.

Conceptual graphic of a nano-scale quantum dot photodetector that shows the CdSe quantum dot linked to the Au electrode via the HDT molecule.

The working principle of the device is based on 3D-0D-3D resonant electron tunneling from the source (3D) to the quantum dot (0D) and finally to the drain (3D). The quantum dot is referred to as a zero-dimensional system because electrons are confined in all three dimensions and the energy levels are quantized. In a three-dimensional system like the electrodes, electrons are free to move and the energy levels form a continuous band. Carrier transport is governed by selection rules involving energy and momentum conservation. The tunneling from the quantum dot to the drain can be enhanced by photo-generated electrons that occupy higher energy levels. This effectively happens when the quantum dot is optically pumped with a light source.

Thus, the current-voltage (IV) characteristics of the device are expected to change under optical pumping, and the device can be utilized as a photodetector. Work to date has consisted of modeling, fabrication and preliminary testing of these devices.

Nano-scale quantum dot photodetectors offer the possibility of nano-scale photodetection for future nano-scale photonic integrated circuits. Other potential photodetector applications of the device include infrared, astronomical, and medical imaging. Future work will include characterization and optimization of the device performance, and integration with other nano-scale quantum dot photonic integrated circuit components. EE

FACULTY ADVISOR: PROFESSOR LIH Y. LIN
COLLABORATORS: PROFESSOR BABAK PARVIZ (EE)
RESEARCH AREA: DEVICES
GRANT/FUNDING SOURCE: UIF/IGERT FELLOWSHIP

Novel Wavelength Selective Switch Based on Electro-Optical Polymer

ANNA PYAYT, GRADUATE STUDENT (EE)

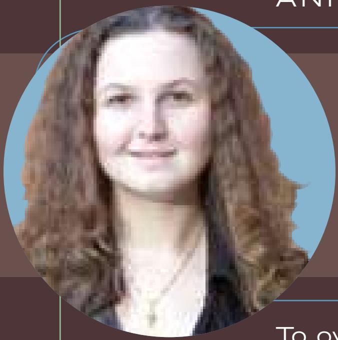

High-speed and high-performance optical switches are required for optical communication and optical signal-processing. Traditional switches without wavelength selectivity still can not satisfy wavelength division multiplexing (WDM) system requirements for the optical signals to be switched at both fiber and wavelength levels. This is a task requiring wavelength selective switching.

To overcome the size and speed limitations of current technologies, a new type of wavelength selective switch based on electro-optic (EO) polymer micro-ring resonators is being developed. The basic switching element is a 2x2 switch with two micro-rings and two intersecting bus waveguides.

Each of the rings under voltage applied can independently couple light of one wavelength and switch it from the Input m to Output n (m≠n, m and n can be 1 or 2). Without coupling to the ring, light propagates from Input m to Output m (m can be 1 or 2). This 2x2 switch can be used as a building block for the larger NxN switches, which can independently switch large number of wavelengths and their combinations from any input to any output. The typical radius of the switching rings is only 25 μm, which makes the overall size of the device two orders of magnitude smaller than traditional switches. The entire NxN switch array can fit on top of a silicon complementary metal-oxide semiconductor (CMOS) circuit chip. It makes fabrication of a single chip optical switch node possible and self contained with all the necessary control electronics. This design uses all the benefits of EO polymer switches and adds extra functionality because of the ability to switch every wavelength independently. Calculation showed that low loss, high isolation and fast switching speed device is possible using existing EO polymers.

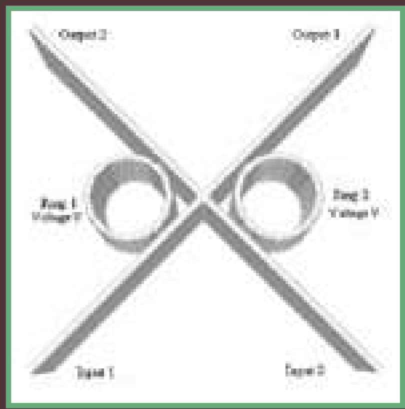

SCHEMATIC STRUCTURE OF THE WAVELENGTH SELECTIVE 2X2 SWITCH.

Theoretical analysis using matrix models and numeric methods have been performed to find optimal device configuration. Preliminary devices have been made from passive polymers using soft lithography. Future efforts will focus on process optimization and the fabrication of the EO polymer devices.EE

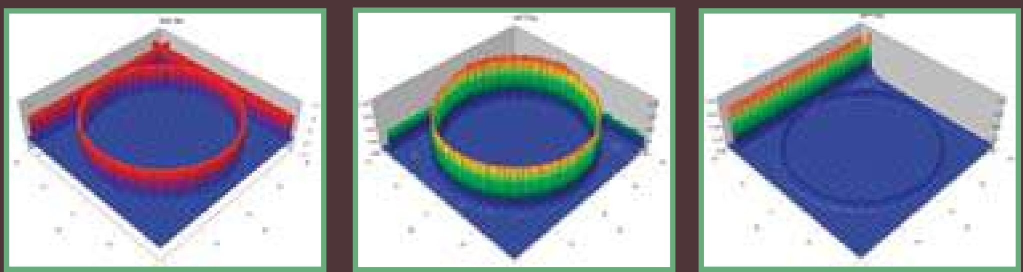

REFRACTIVE INDEX PROFILE AND FDTD SIMULATION OF THE FIELD DISTRIBUTION IN THE “CROSS” AND “BAR” STATES.

FACULTY ADVISOR: PROFESSOR LARRY DALTON (CHEMISTRY) AND ANTAO CHEN (APPLIED PHYSICS LAB)
COLLABORATORS: PROFESSOR ALEX JEN (MATERIAL SCIENCE AND ENGINEERING), AXEL SCHERER (CALTECH)
RESEARCH AREA: PHOTONICS
GRANT/FUNDING SOURCE: NSF

A New Surface Plasmon Resonance Biosensor Based on Diffraction Gratings

FUMIN YANG, GRADUATE STUDENT (EE)

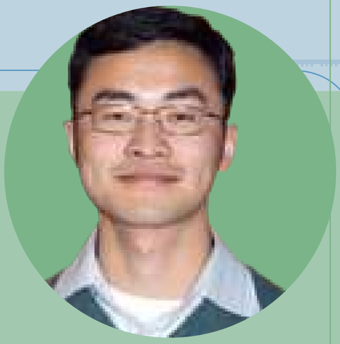

A Surface Plasmon Resonance (SPR) wave can be generated at the interface of a metal and a dielectric through the coupling of the light with either a prism or a diffractive grating structure. The SPR wave property is closely related to the dielectric property in the ambient environment at the interface. This phenomenon is utilized for sensing purposes through the binding of the detection species at the interface.

This project is developing a diffraction grating based SPR sensor, where multiple surface plasmons with different wavelengths are generated through the coupling of a micro-fabricated multi-frequency profile diffractive grating.

There are two main parts to this research: 1. The fabrication of the diffraction grating and its integration into the SPR biosensor, and 2. A modeling tool to simulate light diffraction on a multi-frequency diffraction grating embedded in a multi-layer structure.

Other work involves designing, fabricating and testing the microfluidic liquid sample transfer system for the SPR biosensor. Currently, the single frequency profile diffraction grating is being fabricated, and it's also undergoing the design of its integration into SPR sensors. The models to simulate light propagation through the plane multi-layer structure, and light diffraction on a single frequency profile metallic grating are completed.

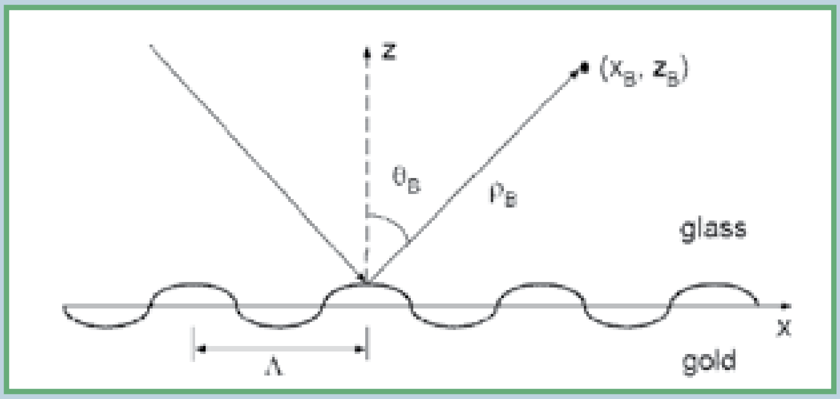

MODEL FOR LIGHT DIFFRACTION ON A SINGLE FREQUENCY PROFILE METALLIC GRATING.

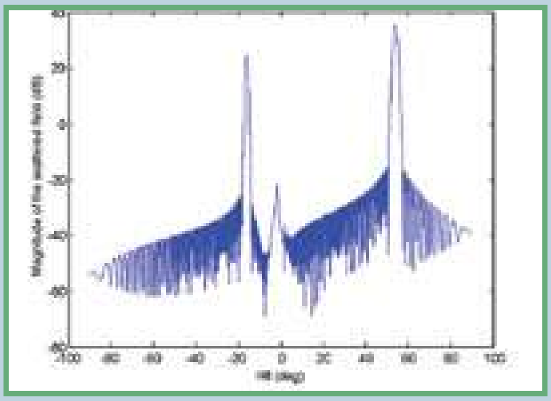

MAGNITUDE OF THE SCATTERED FIELD (IN DB) AT DIFFERENT ANGLES.

Next steps involve fabricating multi-frequency profile diffraction gratings, and testing its effect on the SPR signal. A model for simulation of light diffraction on a multi-frequency diffraction grating embedded in a multi-layer structure will also be built. EE

FACULTY ADVISOR: PROFESSOR ROBERT B. DARLING
COLLABORATORS: PROFESSOR SHAOYI JIANG (ChemE), PROFESSOR JIRI HOMOLA (INSTITUTE OF RADIO ENGINEERING AND ELECTRONICS, ACADEMY OF SCIENCES OF THE CZECH REPUBLIC, PRAGUE)
RESEARCH AREA: DEVICES AND MEMS
GRANT/FUNDING SOURCE: FOOD AND DRUG ADMINISTRATION

Droplet Based Microfluidics on Textured Surfaces

ASHUTOSH SHASTRY, RESEARCH ASSOCIATE (EE)

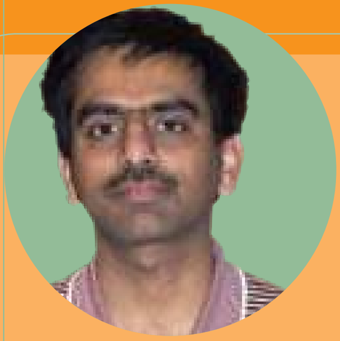

Exciting prospects for lab-on-chip systems have fueled the emergence of droplet-based "digital" microfluidics. Electrowetting, the electrical approach to droplet manipulation, involves actuating droplets on a hydrophobic surface via voltage-controlled lowering of the solid-liquid interfacial tension at one edge of the droplet. However, surface fouling and high actuation voltages impede the development of bioassay systems. To remedy these issues, a novel approach employing microtextured surfaces was envisioned and the enabling modules successfully implemented to lay the foundation for creating a completely reconfigurable, CMOS-compatible bioassay platform.

To overcome the first road block of surface fouling, novel low protein-fouling surfaces with alternating hydrophobic and hydrophilic patterns were developed. Currently, the design, fabrication and initial characterization have been completed. Radio-labeled protein fouling experiments are under way to quantify the fouling.

CONTACT ANGLE MEASUREMENT OF A DROPLET WITH VOLUME 7.68 µl LEADS TO $Ø_f$ = 137° AND THE VOLUME OF DROP IS 7.68 µl. ONE CAN OBSERVE LIGHT BELOW THE DROPLET, CONFIRMING THE HYPOTHESIS THAT THE DROPLET RESTS ON NON-FOULING HYDROPHILIC PILLAR TOPS.

TWO 8 µl DROPLETS WERE PLACED ON OPPOSITELY ORIENTED GRADIENTS ON THE SAME DIE AND VIBRATED. THE DROPLETS TRAVELED IN OPPOSITE DIRECTIONS DOWN THEIR RESPECTIVE MICROTEXTURED SURFACE GRADIENTS, CONFIRMING THAT THE DROPLETS WERE DIRECTED BY THEIR GRADIENTS AND NOT BY BIAS IN VIBRATION.

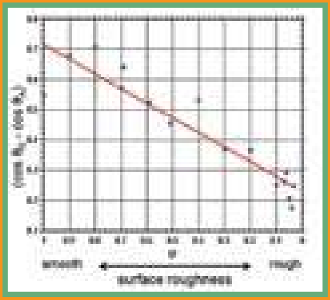

THE IMPEDING FORCE OF CONTACT ANGLE HYSTERESIS IS PROPORTIONAL TO ($COSØ_R$ - $COSØ_A$), THE DIFFERENCE OF RECEDING AND ADVANCING CONTACT ANGLE. AS SEEN IN THE PLOT, THIS FORCE DECREASES AS THE SOLID-LIQUID AREA FRACTION ϕ DECREASES.

Next, systematic variation of roughness was employed to create contact angle gradients that guided droplets propelled by vibration.

The surfaces were designed to maintain air traps beneath the droplet. The dimensions and spacing of the pillars etched in silicon were varied to create the gradient. Thus, solid-liquid contact area fraction was introduced as a new control variable in any scheme of manipulating droplets.

A driving force is required to mitigate the impeding force due to pinning of the three phase contact line. A low force requirement translates to a low actuation voltage for electrowetting. The impeding force decreased with the solid-liquid contact area, and shows promising results in overcoming high actuation voltages. Texture dependence of the impeding force (hysteresis) is shown at bottom left.

By creating non-fouling surfaces, electrowetting based bioassay systems are made possible. Guiding droplets down "hard coded" textured tracks lowering the impeding force through texturing have been demonstrated. Next steps include replacing acoustic actuation by electrical means, and establishing the feasibility of low voltage programmable gradients. EE

FACULTY ADVISOR: PROFESSOR KARL BÖHRINGER
COLLABORATORS: SIDDHARTHA GOYAL, MARIANNE CASE (RESEARCH ENGINEER), AZIEL EPILEPSIA (GRADUATE STUDENT)
RESEARCH AREA: MICROFLUIDICS/MEMS
GRANT/FUNDING SOURCE: NIH/MLSC

Self-Assembling Silicon

CHRIS MORRIS, GRADUATE STUDENT (EE)

For integrated circuit devices, the performance of each new technology generation benefits from a reduction in size. Robotic assembly and packaging integrates these devices into useful products. However, the miniaturization of final device packages may be limited by the use of such serial, robotic handling methods.

Using top-down microfabrication methods to create devices, as well as self-assembly to create 3-D functional structures out of these devices will help overcome these limitations. This requires the four following items: 1) the development of new microfabrication technologies compatible with existing methods to create parts that can participate in self-assembly, 2) "programming" the assembly of these parts 3) agitation of the system to encourage intended assembly, and 4) the creation of permanent mechanical and/or electrical connections.

This research aims to self-assemble silicon-based, 3-D functional devices, and fabricate new, lower-cost systems by assembling pre-microfabricated parts in different ways. New microfabrication technologies for parts have been developed and "programmed" to assemble using surface energy modifications and capillary forces.

By combining microfabrication and chemical handling techniques, micrometer-scale parts have been developed with silicon-on-insulator (SOI) wafers.

Photolithography and deep reactive ion etches define each part, and hydrofluoric (HF) acid etching releases parts into a carrier fluid. The sidewalls of each part are programmed by rendering surfaces hydrophobic or hydrophilic with molecular self-assembled monolayers. The resulting surface energies program the assembly by determining the wetability of a hydrophobic adhesive. The part faces then coat with this hydrophobic adhesive and adhere to each other by capillary forces. Gentle tumbling acts as agitation, cross-linking the hydrophobic polymer adhesive with heat to form permanent mechanical bonds.

By quantifying the agitation energy and correlating the energy of individual bonds, it is expected that control over this type of self-assembly will improve in the future, and many exciting device architectures will result. EE

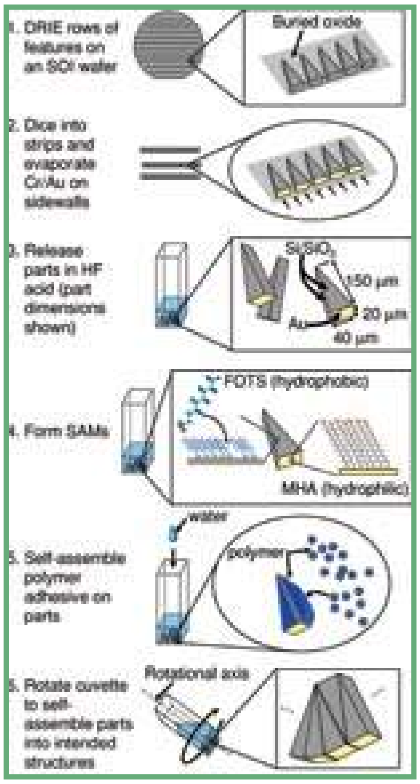

FABRICATION PROCESS FOR TRIANGULAR MICROSTRUCTURES THAT SELF-ASSEMBLE. THE PROCESS INVOLVES SEVERAL SELF-ASSEMBLY STEPS, SUCH AS THE SELF-ASSEMBLED-MONOLAYER (SAM) IN STEP 4, THE SELF-ASSEMBLY OF POLYMER ADHESIVE IN STEP 5, AND SELF-ASSEMBLY OF THE PARTS IN STEP 6.

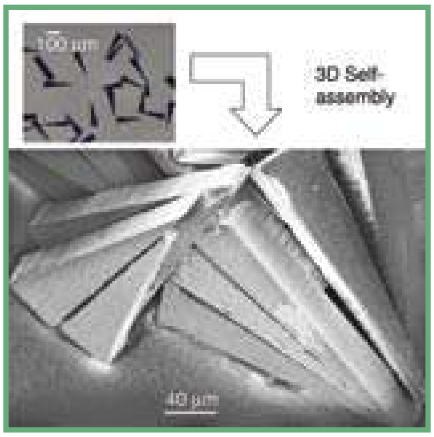

A 3-D SELF-ASSEMBLED STRUCTURE FORMATION. UNASSEMBLED STRUCTURES AT AIR/WATER INTERFACE SHOWN ON TOP. STRUCTURES IMMERSED IN WATER WITH CURED POLYMER ADHESIVE SHOWN AT BOTTOM (FROM MORRIS, C. J., HO., H, AND PARVIZ, B. A., "BRIDGING BETWEEN NANO- AND MICRO-SCALES FOR SYSTEM INTEGRATION: CONTROLLED CAPILLARY FORCE-DRIVEN SELF ASSEMBLY," 5TH IEEE CONFERENCE ON NANOTECHNOLOGY, NAGOYA, JAPAN, JULY 11-15, 2005, PP.508-511). ©2005 IEEE.

FACULTY ADVISOR: PROFESSOR BABAK PARVIZ
RESEARCH AREA: DEVICES AND MEMS
GRANT/FUNDING SOURCE: DARPA, DOD FELLOWSHIP

Self Assembly for Parallel Packaging of Micro Devices

JIANDONG FANG, GRADUATE STUDENT (EE)

Aiming for a stand-alone operation, a typical micro device is an integrated system containing components from different technologies such as CMOS and MEMS. Monolithic fabrication of such a hybrid system is greatly challenged by process incompatibilities. Self-assembly techniques enable fast and parallel integrating and packaging of heterogeneous components.

Based on the principle for delivering micro components to receptor sites, the self-assembly techniques derived by the MEMS Lab at UW EE can be classified into three categories: capillary-driven self-assembly, feature-directed self-assembly, and a combination of shape-directed and capillary-driven self-assembly. These techniques satisfy the manufacturing requirements for micro devices ranging in application from biochemical analysis, to radio frequency identification (RFID), to micromechanical transducers with moving components.

A capillary-driven self-assembly process mounts micro components onto a substrate via adhesive droplets on the binding sites, and alignment with submicron accuracy can be achieved by interfacial energy minimization. By using this assembly method and heating polymerizable adhesive liquid, piezo actuators for micro fluidic pumps were assembled.

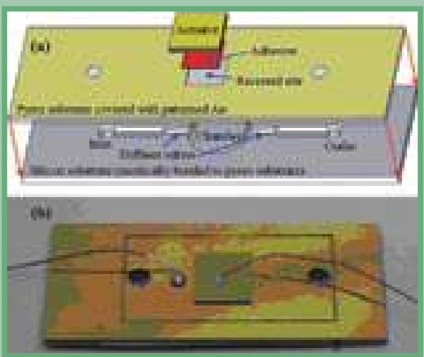

A 4MM SQUARE PIEZO ACTUATOR MOUNTED AT THE CENTER OF THE CHAMBER DIAPHRAGM OF A MICRO PUMP. (A) A SCHEMATIC EXPLODED VIEW. (B) AN OPTICAL IMAGE (THIN ELECTRICAL WIRES SOLDERED TO THE ACTUATOR'S TOP SURFACE AND THE SUBSTRATE, UNDERNEATH THE ACTUATOR IS A CAVITY FILLED WITH ADHESIVE THAT AFFIXES THE ACTUATOR'S BOTTOM EDGES AGAINST THE SUBSTRATE).

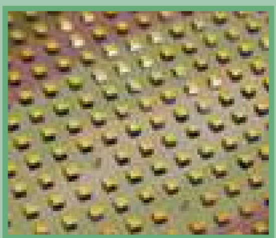

1MM SQUARE SILICON PARTS SELF-ASSEMBLED ON A SUBSTRATE WITH UNIQUE IN-PLANE ORIENTATIONS BY TWO-STAGE FEATURE RECOGNITION; CIRCULAR FEATURES FOR THE 1ST STAGE, AND CROSS FEATURES FOR THE 2ND STAGE.

Feature-directed self-assembly is based on feature recognition between protruding and recessed features on components and receptor sites. Micro components are driven by centrifugal forces from orbital shaking until their features fall into trenches on a substrate. Uniquely orienting self-assembly is achieved by two-stage feature recognition.

Mounting of components with controlled poses (vertical or horizontal) is achieved by combining shape recognition and capillary-driven self-assembly. Shape recognition allows micro components to stand vertically in apertures on a vibrating plate. Micro components can then lie down and self-align to receptor sites by capillary forces.

The capillary-driven self-assembly of piezo actuators has significant advantages over the conventional bonding method with silver epoxy. The uniquely orienting assembly enables flip-chip bonding of micro chips with multiple asymmetrical interconnects. The vertical mounting technique is useful for RF and optical MEMS components. EE

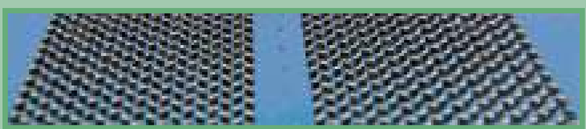

790μM SQUARE SILICON PARTS STAND VERTICALLY IN APPROPRIATELY DESIGNED APERTURES ON THE SILICON SUBSTRATE.

FACULTY ADVISOR: PROFESSOR KARL F. BÖHRINGER
RESEARCH AREA: MEMS
GRANT/FUNDING SOURCE: NIH CENTER OF EXCELLENCE IN GENOMIC SCIENCES & TECHNOLOGY

NEW STUDENT RESOURCES CENTER

After two years of renovation, the newly updated Sieg Hall was officially opened to the public. Members of UW EE and The College of Engineering attended a ribbon cutting ceremony on October 21st, 2005. In addition to structural repairs to the building itself, the following space has been provided to UW EE students:

- INTEGRATED STUDENT CENTER – a designated area where students can study, discuss EE related issues, or socialize
- OFFICES FOR STUDENT-RUN ORGANIZATIONS – separate dedicated office space for IEEE, HKN, and GSA
- TA CENTER – individual workspace for each TA as well as a computer lab
- TUTORIAL CENTER – A room which holds up to 24 students along with three additional smaller and adjoining "break-out" rooms

ACTING DEAN MANI SOMA OFFICIALLY OPENS SIEG HALL AT RIBBON CUTTING CEREMONY.

TEKTRONIX UNDERGRADUATE RESEARCH LAB

On November 18, 2005, the Department of Electrical Engineering celebrated the opening of our first lab solely dedicated to undergraduate research opportunities. The Tektronix Undergraduate Research Lab in Sieg Hall was made possible through the generous support of Tektronix, Inc. Tektronix gave over $350,000 worth of the equipment and furniture needed to fully outfit the lab. Students who are serious about research opportunities during their undergraduate years can now work in a dedicated facility on state-of-the-art equipment. Thank you Tektronix!

FROM LEFT TO RIGHT: DAVID BROWN, VICE PRESIDENT OF CENTRAL ENGINEERING AT TEKTRONIX (UWEE ALUM '76), STAN KAVECKIS, PRINCIPAL ENGINEER AT TEKTRONIX (UWEE ALUM '72), AND JIM BROPHY, LOCAL SALES ACCOUNT MANAGER AT TEKTRONIX

EE UNDERGRADUATE JAMES HAMMER RECEIVES A LESSON FROM JIM BROPHY ON HOW TO USE THE EQUIPMENT.

IN MEMORY OF BOB CLARK

The Department was saddened by the death of Professor Robert N. Clark on January 27, 2006. Professor Clark joined the EE Department in 1957 from Honeywell Inc. where he had established his reputation as an expert in the analysis of feedback systems and automatic control. This emergent technology was critical to the challenges of the times including the understanding of the dynamics of complex systems, from motors to aircraft, and the design of the necessary control systems. He documented his expertise in a seminal text, "Introduction to Automatic Control Systems" published by John Wiley and Sons in 1962 that had at least three printings. This book was particularly impressive for the relevance of its content. Students were challenged with real-world examples from Bob's experience, lending more excitement to their study than is often the case in introductory texts. Upon arriving at the University of Washington, Bob was an early and major contributor in developing our curriculum in systems and automatic control.

Professor Clark received his BSEE and MSEE degrees from the University of Michigan (1950 and 1951) and his Ph.D. from Stanford University in 1969 while on leave from our department. His expertise was recognized nationally and internationally by his election as a Fellow of the IEEE in 1983 with the citation: "For contributions to engineering education and the practical application of control theory." He was also appointed Professor of Aeronautics and Astronautics in 1988 and continued to serve both departments until his retirement in 1994.

Those of us who served in the Department with Bob enjoyed his wry humor and, especially, his generous friendship. Bob and his wife Mary were gracious and dedicated members of the Electrical Engineering community who provided ready hospitality to faculty and students. EE

EE FACULTY

Afromowitz, Marty
Professor
Microtechnology/Sensors
Ph.D., 1969 Columbia University
NIH Career Development Award

Allstot, David
Professor & Chair
System-on-Chip VLSI
Ph.D., 1979 UC-Berkeley
IEEE Fellow

Ammer, Josie
Assistant Professor
Circuits and Algorithms for Wireless Communication
Ph.D., 2005 UC-Berkeley

Atlas, Les
Professor
Signal and Image Processing
Ph.D., 1984 Stanford University
NSF Presidential Young Investigator
IEEE Fellow

Bilmes, Jeff
Associate Professor
Signal and Image Processing
Ph.D., 1999 UC-Berkeley
NSF CAREER Award

Böhringer, Karl
Associate Professor
Microelectromechanical Systems (MEMS)
Ph.D., 1997 Cornell University
NSF CAREER Award

Bushnell, Linda
Research Assistant Professor
Controls and Robotics
Ph.D., 1994 UC-Berkeley
NSF ADVANCE Fellow

Chen, Tai-Chang
Research Assistant Professor
MEMS and Microfabrication
Ph.D., 1997 University of Washington

Chinowsky, Tim
Research Assistant Professor
Sensors, Instumentation, Analog Electronics
Ph.D., 2000 University of Washington

Chizeck, Howard
Professor
Controls and Robotics
Sc.D., 1982 MIT
IEEE Fellow

Christie, Rich
Associate Professor
Energy Systems
Ph.D., 1989 Carnegie Mellon University
NSF Presidential Young Investigator

Crum, Lawrence
Research Professor
Medical Ultrasound
Ph.D., 1967 Ohio University
ASA Fellow

Dailey, Daniel J.
Research Professor
Intelligent Transportation Systems
Ph.D., 1988 University of Washington

Damborg, Mark
Professor
Energy Systems
Ph.D., 1969 University of Michigan

Darling, R. Bruce
Professor
Devices, Circuits, and Sensors
Ph.D., 1985 Georgia Institute of Technology

Dunham, Scott
Professor
Materials and Devices
Ph.D., 1985 Stanford University

El-Sharkawi, Mohamed
Professor
Intelligent Systems and Energy
Ph.D., 1980 University of British Columbia
IEEE Fellow

Goldstein, Evan
Affiliate Professor
Lightwave Communications
Ph.D., 1989 Columbia University
IEEE Fellow, OSA Fellow

Gupta, Maya
Assistant Professor
Signal Processing
Ph.D., 2003 Stanford University

Hannaford, Blake
Professor
Biorobotics
Ph.D., 1985 UC-Berkeley
NSF Presidential Young Investigator, IEEE EMBS Early Career Achievement Award, IEEE Fellow

Hauck, Scott
Associate Professor
VLSI and Digital Systems
Ph.D., 1995 University of Washington
NSF CAREER Award, Sloan Research Fellowship

Holl, Mark
Research Assistant Professor
MEMS, Micro-total analytical systems
Ph.D., 1995 University of Washington

Hwang, Jenq-Neng
Professor
Signal and Image Processing
Ph.D., 1988 University of Southern California
IEEE Fellow

Jandhyala, Vikram
Associate Professor
Electromagnetics, Fast Algorithms, Devices
Ph.D., 1998 University of Illinois
NSF CAREER Award

Kim, Yongmin
Professor/Chair of Bioengineering
Digital Systems, Image Processing and Medical Imaging
Ph.D., 1982 University of Wisconsin - Madison
IEEE Fellow, IEEE/EMBS Early Career Achievement Award

Kirchhoff, Katrin
Research Assistant Professor
Multilingual Speech Processing, Machine Learning
Ph.D., 1999 University of Bielefeld

Klavins, Eric
Assistant Professor
Controls and Robotics
Ph.D., 2001 University of Michigan
NSF CAREER Award

Kuga, Yasuo
Professor
Electromagnetics
Ph.D., 1983 University of Washington
NSF Presidential Young Investigator Award
IEEE Fellow

Lin, Lih
Associate Professor
Photonics, MEMS
Ph.D., 1996 UC-Los Angeles

Liu, Hui
Associate Professor
Communications and Signal Processing
Ph.D., 1985 University of Texas, Austin
NSF CAREER Award, ONR Young Investigator

Mamishev, Alex
Associate Professor
Electric Power Systems, MEMS, Sensors
Ph.D., 1999 MIT
NSF CAREER Award

McMurchie, Larry
Research Assistant Professor
VLSI and Digital Systems
Ph.D., 1977 University of Washington

Meldrum, Deirdre
Professor
Genome Automation
Ph.D., 1993 Stanford University
Presidential Early Career Award (PECASE), NIH SERCA Award
AAAS Fellow, IEEE Fellow

Nelson, Brian
Research Associate Professor
Plasma Physics
Ph.D., 1987 University of Wisconsin - Madison

Ostendorf, Mari
Professor
Signal and Image Processing
Ph.D., 1985 Stanford University
IEEE Fellow

Otis, Brian
Assistant Professor
RF/Analog IC Design
Ph.D., 2005 UC-Berkeley

Parviz, Babak
Assistant Professor
Microelectromechanical Systems (MEMS)
Ph.D., 2001 University of Michigan

Peckol, James S.
Lecturer
Digital Systems
Ph.D., 1985 University of Washington

Poovendran, Radha
Assistant Professor
Communications Networks and Security
Ph.D., 1999 University of Maryland
NSA Rising Star Award, NSF CAREER Award, ARO YIP and ONR YIP Awards, PECASE Award

Ramon, Ceon
Research Scientist, Lecturer
Electromagnetics and Remote Sensing
Ph.D., 1973 University of Utah

Riskin, Eve
Professor & Associate Dean
Signal and Image Processing
Ph.D., 1990 Stanford University
NSF Presidential Young Investigator, Sloan Research Fellowship

Ritcey, Jim
Professor
Communications and Signal Processing
Ph.D., 1985 UC - San Diego

Rosen, Jacob
Research Assistant Professor
Biorobotics, Human-Machine Interfaces
Ph.D., 1997 Tel-Aviv University

Roy, Sumit
Professor & Associate Chair for Research & Development
Communications and Networking
Ph.D., 1988 UC - Santa Barbara

Sahr, John
Professor
Electromagnetics and Remote Sensing
Ph.D., 1990 Cornell University
NSF Presidential Young Investigator, URSI Booker Fellow, URSI Young Scientist Award

Shapiro, Linda
Professor
Signal and Image Processing
Ph.D., 1974 University of Iowa
IEEE Fellow, IAPR Fellow

Shi, C.J. Richard
Professor
VLSI and Digital Systems
Ph.D., 1994 University of Waterloo
NSF CAREER Award, IEEE Fellow

Soma, Mani
Professor & Acting Dean of Engineering
Mixed Analog-Digital System Testing
Ph.D., 1980 Stanford University
IEEE Fellow

Spindel, Robert
Professor
Signal Processing/Ocean Acoustics
Ph.D., 1971 Yale University
IEEE Fellow, ASA Fellow, MTS Fellow, A.B. Wood Medal, IEEE Oceanic Engineering Society Technical Achievement Award

Strunz, Kai
Assistant Professor
Electric Power Systems and Power Electronics
Ph.D., 2001 Saarland University
NSF CAREER Award

Sun, Ming-Ting
Professor
Signal and Image Processing
Ph.D., 1985 UC-Los Angeles
IEEE Fellow

Tsang, Leung
Professor & Associate Chair for Education
Electromagnetics, Remote Sensing
Ph.D., 1976 MIT
IEEE Fellow, OSA Fellow

Wilson, Denise
Associate Professor
Circuits and Sensors
Ph.D., 1995 Georgia Institute of Technology
NSF CAREER Award

Yee, Sinclair
Professor
Photonics, Sensors
Ph.D., 1965 UC – Berkeley
IEEE Fellow

Zick, Greg
Professor
VLSI and Digital Systems
Ph.D., 1974 University of Michigan

EMERITI

Albrecht, Robert
Controls and Robotics
Ph.D., 1961 University of Michigan

Alexandro, Frank
Controls and Robotics
Eng.Sc.D., 1964 New York University

Andersen, Jonny
Circuits and Sensors
Ph.D., 1965 MIT

Bjorkstam, John L.
Controls and Robotics
Ph.D., 1958 University of Washington

Dow, Daniel G.
Ph.D., 1958 Stanford University

Guilford, Edward C.
Ph.D., 1960 UC-Berkeley

Haralick, Robert
Signal and Image Processing
Ph.D., 1969 University of Kansas
IEEE Fellow

Helms, Ward
Circuits and Sensors
Ph.D., 1968 University of Washington

Hsu, Chih-Chi
Ph.D., 1957 Ohio State University

Ishimaru, Akira
Electromagnetics and Waves in Random Media
Ph.D., 1958 University of Washington
IEEE Fellow, OSA Fellow, IOP Fellow, IEEE Heinrich Hertz Medal, URSI John Dillinger Medal and Member, National Academy of Engineering

Jackson, Darrell
Ph.D., 1977 California Institute of Technology

Johnson, David L.
Ph.D., 1955 Purdue University

Lauritzen, Peter O.
Ph.D., 1961 Stanford University

Lewis, Laurel
Ph.D., 1947 Stanford Unversity

Moritz, William E.
Ph.D., 1969 Stanford University

Noges, Endrik
Ph.D., 1959 Northwestern University

Peden, Irene
Ph.D., 1962 Stanford University
NSF "Engineer of the Year" Member, National Academy of Engineering, IEEE Fellow, IEEE Harden Pratt Award, U.S. Army Outstanding Civilian Service Medal

Porter, Robert B.
Ph.D., 1970 Northeastern University
ASA Fellow, OSA Fellow

Potter, William
MSEE, 1959 US Naval Postgraduate School

Redeker, Charles C.
Ph.D., 1964 University of Washington

Sigelmann, Rubens A.
Ph.D., 1963 University of Washington

CONGRATULATIONS TO JEFF BILMES, VIKRAM JANDHYALA AND ALEX MAMISHEV WHO WERE RECENTLY PROMOTED TO ASSOCIATE PROFESSORS.

WE APOLOGIZE FOR ANY ERRORS, OMISSIONS OR MISSPELLINGS IN 2006 EEK. WE WOULD LIKE TO EXTEND SPECIAL APPRECIATION TO THE FACULTY, STAFF AND STUDENTS WHO ASSISTED IN PRODUCING THIS PUBLICATION AND TO THE SPONSORS WHOSE GENEROSITY MADE IT POSSIBLE.

CORRECTION TO EEK 2005

THE EDITORS OF EEK WOULD LIKE TO APOLOGIZE FOR THE ERROR FOUND ON PAGE 11 OF EEK 2005. THE GRAPHIC ON THIS PAGE SHOULD BE CREDITED AS FOLLOWS: © JAMSTEC.

PHOTO TAKEN BY UW BIOENGINEERING PROFESSOR, BUDDY RATNER.

www.ee.washington.edu

University of Washington
Department of Electrical Engineering
Paul Allen Center — Room AE100R
Campus Box 352500
Seattle, Washington 98195-2500